

AD-A172 522

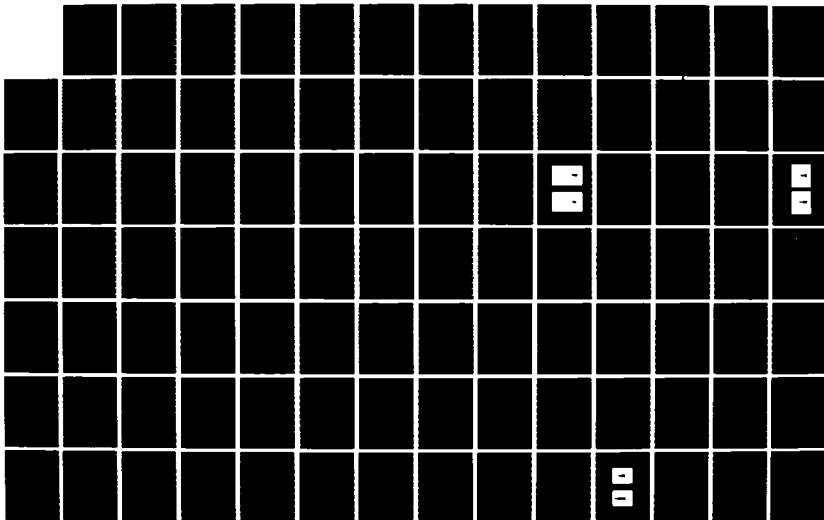
INVESTIGATION OF FUEL ADDITIVE EFFECTS ON SOOTING  
FLAMES(U) UNITED TECHNOLOGIES RESEARCH CENTER EAST  
HARTFORD CT P A BOMCZYK 31 JUL 86 UTRC/R86-956545-F  
AFOSR-TR-86-0051 F49620-83-C-0113

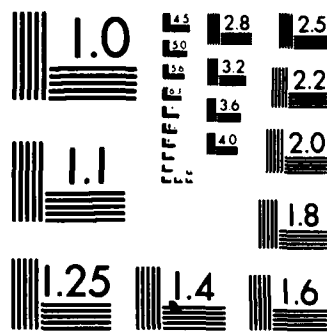
1/2

UNCLASSIFIED

F/G 21/4

NL





MICROCOPY RESOLUTION TEST CHART  
NATIONAL BUREAU OF STANDARDS 1963 A

(2)

R86-956545-F

Investigation of Fuel Additive Effects on Sooting Flames

Approved for public release;  
distribution unlimited.

by

AIR FORCE OFFICE OF SCIENTIFIC RESEARCH (AFSC)  
NOTICE OF TRANSMITTAL TO DTIC  
This technical report has been reviewed and is  
approved for public release IAW AFR 190-12.  
Distribution is unlimited.  
MATTHEW J. KERPER  
Chief, Technical Information Division

P. A. Bonczyk

United Technologies Research Center

East Hartford, Conn. 06108

July 31, 1986

Final Technical Report

under

Contract F49620-83-C-0113

DTIC  
ELECTE  
OCT 2 1986  
S A

Prepared for

Air Force Office of Scientific Research

Bolling Air Force Base, DC 20332

AD-A172 522

DTIC FILE COPY

AD 4172 522

# REPORT DOCUMENTATION PAGE

1a REPORT SECURITY CLASSIFICATION <b>Unclassified</b>			1b RESTRICTIVE MARKINGS		
2a SECURITY CLASSIFICATION AUTHORITY			3 DISTRIBUTION/AVAILABILITY OF REPORT Distribution unlimited; approved for public release		
2b DECLASSIFICATION/DOWNGRADING SCHEDULE					
4 PERFORMING ORGANIZATION REPORT NUMBER(S) <b>R86-956545-F</b>			5 MONITORING ORGANIZATION REPORT NUMBER(S) <b>AFOSR-TR. 86-0851</b>		
6a NAME OF PERFORMING ORGANIZATION <b>United Technologies Research Center</b>		6b OFFICE SYMBOL (if applicable)	7a NAME OF MONITORING ORGANIZATION <b>Air Force Office of Scientific Research</b>		
6c ADDRESS (City, State, and ZIP Code) <b>East Hartford, CT 06108</b>		7b ADDRESS (City, State, and ZIP Code) <b>Bolling AFB DC 20332-6448</b>			
8a NAME OF FUNDING/SPONSORING ORGANIZATION <b>Air Force Office of Sci. Res.</b>		8b OFFICE SYMBOL (if applicable) <b>AFOSR/NA</b>	9 PROCUREMENT INSTRUMENT IDENTIFICATION NUMBER <b>F49620-83-C-0113</b>		
9a ADDRESS (City, State, and ZIP Code) <b>Bolling AFB DC 20332-6448</b>		10 SOURCE OF FUNDING NUMBERS			
		PROGRAM ELEMENT NO <b>61102F</b>	PROJECT NO <b>2308</b>	TASK NO <b>A2</b>	WORK UNIT ACCESSION NO
11 TITLE (Include Security Classification) <b>Investigation of Fuel Additive Effects on Sooting Flames (Unclassified)</b>					
12 PERSONAL AUTHOR(S) <b>Bonczyk, Paul A.</b>					
13a TYPE OF REPORT <b>Final</b>		13b TIME COVERED FROM <b>5/1/83</b> TO <b>5/31/86</b>		14 DATE OF REPORT (Year, Month, Day) <b>July 31, 1986</b>	
15 PAGE COUNT <b>128</b>					
16 SUPPLEMENTARY NOTATION					
17 COSATI CODES			18 SUBJECT TERMS (Continue on reverse if necessary and identify by block number)		
FIELD	GROUP	SUB-GROUP			
<b>21</b>	<b>01</b>		<b>Additive, Alkaline-Earth, Ferrocene, Flame, Soot</b>		
<b>21</b>	<b>02</b>				
19 ABSTRACT (Continue on reverse if necessary and identify by block number) The objective of this research was to clarify the mechanisms responsible for the suppression of soot in flames by selected fuel additives. Measurements were limited to well-defined hydrocarbon/air gaseous- and prevaporized liquid-fueled diffusion flames. Emphasis was given to alkaline-earth salt additives in an ethylene/air flame, as well as to ferrocene in a flame fueled by a prevaporized toluene/iso-octane mixture. Nonperturbing laser/optical diagnostic techniques were used to measure flame temperature, as well as to relate changes in soot particulate size, number density, and volume fraction to additive type and concentration. For the ethylene flame, additive effectiveness was shown to vary from point-to-point in the flame and to maximize in the direction of increasing flame temperature. From the latter, and measured concentrations of metal combustion species, MOH <sup>+</sup> (M = Ba, Sr, etc.) were concluded to be the particular species critical to soot suppression. The data indicate					
20 DISTRIBUTION/AVAILABILITY OF ABSTRACT <input checked="" type="checkbox"/> UNCLASSIFIED/UNLIMITED <input type="checkbox"/> SAME AS RPT <input type="checkbox"/> DTIC USERS			21 ABSTRACT SECURITY CLASSIFICATION <b>Unclassified</b>		
22a NAME OF RESPONSIBLE INDIVIDUAL <b>Julian M. Tishkoff</b>			22b TELEPHONE (Include Area Code) <b>(202) 767-4935</b>		22c OFFICE SYMBOL <b>AFOSR/NA</b>

UNCLASSIFIED

SECURITY CLASSIFICATION OF THIS PAGE

additive intervention at both early and late stages of soot formation, but it was not possible to conclude early intervention firmly. For the alkaline-earths, an experiment complementary to the foregoing was conducted to test an often quoted hypothesis of soot suppression in which metal-induced increases in OH concentration are presumed to enhance soot oxidation and removal. This was found, however, not to be valid. The effect of the alkaline-earths on OH was to decrease the concentration of the latter radical at all points in the ethylene/air flame, which fundamentally is not supportive of the preceding hypothesis. For the toluene flame, ferrocene was observed to suppress a visible soot plume completely. Mie scattering measurements at a late combustion stage demonstrated that suppression results almost entirely from particulate number density reduction.

UNCLASSIFIED

SECURITY CLASSIFICATION OF THIS PAGE

## ILLUSTRATIONS

<u>Figure</u>		<u>Page</u>
1	Symmetric Diffusion Flame Burner	6
2	Lateral Variation of Sodium Atom Concentration	9
3	Soot Size Dependence on Additive Concentration	10
4	Soot Volume Fraction Dependence on Additive Concentration	11
5	Barium Seeded Ethylene/Air Flame Spectra	14
6	Laser Excited OH Fluorescence Spectrum	17
7	Saturated Laser Excited OH Fluorescence	19
8	Lateral Dependence of Flame Temperature	20
9	Barium Suppression of OH Concentration	21
10	Light Polarization Dependence on Particulate Size	26
11	Light Scattering/Extinction Ratio Dependence on Particulate Size	27
12	Size Dependent Light Intensity Ratios vs Additive Concentration	28
13	Soot Reduction with Fuel Additive for Wick Flame	31
14	Porous Cylinder Diffusion Flame	33
15	Soot Reduction with Fuel Additive for Pre vaporized Liquid-Fueled Flame	35
16	Additive Effectiveness on Diameter	37
17	Additive Effectiveness on Number Density	38
18	Additive Effectiveness on Volume Fraction	39
19	Additive Effectiveness on Scattered Light Intensity	40



Distribution/	
Availability Codes	
Avail. and/or	
Dist	Special
AI	

Investigation of Fuel Additive Effects on Sooting Flames

## TABLE OF CONTENTS

	<u>Page</u>
REPORT DOCUMENTATION . . . . .	i
LIST OF ILLUSTRATIONS . . . . .	iii
ABSTRACT . . . . .	1
INTRODUCTION . . . . .	2
ALKALINE-EARTH MEASUREMENTS . . . . .	5
IRON MEASUREMENTS . . . . .	23
WOLFARD-PARKER FLAME . . . . .	23
WICK FLAME . . . . .	29
POROUS CYLINDER FLAME . . . . .	32
PREVAPORIZED LIQUID-FUELED FLAME . . . . .	34
DISCUSSION . . . . .	41
ALKALINE-EARTH ADDITIVES . . . . .	41
IRON ADDITIVES . . . . .	43
FUTURE RESEARCH PLANS . . . . .	43
REFERENCES . . . . .	46
APPENDIX I - SUPPRESSION OF SOOT IN FLAMES BY ALKALINE-EARTH AND OTHER METAL ADDITIVES . . . . .	I-1
APPENDIX II - THE INFLUENCE OF ALKALINE-EARTH ADDITIVES ON SOOT AND HYDROXYL RADICALS IN DIFFUSION FLAMES . . . . .	II-1
APPENDIX III - ADDITIVE EFFECTS ON SOOT IN PREVAPORIZED LIQUID FUELED FLAMES . . . . .	III-1
APPENDIX IV - PRESENTATIONS/PUBLICATIONS UNDER AFOSR CONTRACT F49620-83-C-0113 . . . . .	IV-1

## ABSTRACT

Under Contract F49620-83-C-0113 sponsored by the Air Force Office of Scientific Research, the United Technologies Research Center (UTRC) has conducted research to clarify the mechanisms responsible for the suppression of soot in flames by selected fuel additives. Measurements were limited to well-defined hydrocarbon/air gaseous- and prevaporized liquid-fueled diffusion flames. Emphasis was given to alkaline-earth salt additives in an ethylene/air flame, as well as to ferrocene in a flame fueled by a prevaporized toluene/iso-octane mixture. Nonperturbing laser/optical diagnostic techniques were used to measure flame temperature, as well as to relate changes in soot particulate size, number density, and volume fraction to additive type and concentration. For the ethylene flame, additive effectiveness was shown to vary from point-to-point in the flame and to maximize in the direction of increasing flame temperature. From the latter, and measured concentrations of metal combustion species,  $MOH^+$  ( $M = Ba, Sr, \text{etc.}$ ) were concluded to be the particular species critical to soot suppression. The data indicate additive intervention at both early and late stages of soot formation, but it was not possible to conclude early intervention firmly. For the alkaline-earths, an experiment complementary to the foregoing was conducted to test an often quoted hypothesis of soot suppression in which metal-induced increases in OH concentration are presumed to enhance soot oxidation and removal. This was found, however, not to be valid. The effect of the alkaline-earths on OH was to decrease the concentration of the latter radical at all points in the ethylene/air flame, which fundamentally is not supportive of the preceding hypothesis. For the toluene flame, ferrocene was observed to suppress a visible soot plume completely. Mie scattering measurements at a late combustion stage demonstrated that suppression results almost entirely from particulate number density reduction.



## INTRODUCTION

Particulate soot is a combustion product whose occurrence is highly undesirable in almost all instances. From the military's perspective, for example, soot creates a visible aircraft exhaust plume, thereby rendering the aircraft and its mission vulnerable to an adversary. Secondly, soot may shorten engine life by excessively increasing heat transfer to critical engine components. The use of fuel additives to control soot formation is a proven, effective approach to the problem. It is a simpler alternative than undertaking radical engine redesign for the purpose of reducing soot. The difficulty with additives is that their mechanism(s) of action are very poorly

understood at present, which impedes much more effective and widespread use of them in fuels. The objective of this contract research, expressed in its simplest and most direct terms, was to seek to understand the latter mechanisms, and therefrom find ways to enhance and optimize fuel additive use for soot suppression.

In the recent past, experiments have been carried out to determine the soot suppressing properties of fuel additives in both small well-defined-laboratory flames as well as in more practical combustion media. A reasonably recent compendium of these results has been given by Howard and Kausch (Ref. 1). With perhaps one or two exceptions (Ref. 2), the past experiments have been very qualitative in nature, amounting to a cataloguing of the relative effectiveness of a large number of different additives. Moreover, the measurement techniques were either intrusive by nature or restricted to postflame analysis of soot with and without fuel additives present. Although this genre of additive research is useful in a practical sense, and is a reasonable point of departure for understanding additive behavior, it alone is insufficient for clarifying additive behavior in detail. In order for this to

ensue, more comprehensive and specific measurements are required using experimental techniques which are preferably in-situ in nature.

In order to address the needs mentioned above, the unique approach which was taken was to seek to comprehend the behavior of fuel additives in flames by, insofar as possible, relying upon non-intrusive and spatially precise laser/optical techniques. The latter permit measurements to be made throughout an unperturbed flame. More specifically, the techniques employed included: elastic, Mie scattering of visible laser light to determine soot particulate size, number density and volume fraction with and without an additive present (Ref. 3); optical emission (Ref. 4) and absorption; laser-induced fluorescence (Ref. 5) to both identify and measure the concentrations of additive derived or other flame species; sodium line reversal to determine flame temperature.

Unlike many past experiments, emphasis in this contract research centered on only a few different additives. Specifically, attention was given to the alkaline-earth metals (Ca, Sr and Ba) and to iron. These metals were selected for study since, qualitatively, they were known from past gaseous- and liquid-fueled flame measurements to be effective soot suppressants in both research and practical media (Ref. 1). Second, and equally important, details of their behavior were not understood.

The major portion of the three-year contract period, roughly eighty percent, was devoted to the alkaline-earths, with the remaining time having been allotted to iron. This was not planned initially; instead, more equal emphasis was envisioned. This disparity resulted from the conviction that the alkaline-earth measurements should be brought to a significant state of conclusion, and meeting this objective simply required more time than

R86-956545-F

initially anticipated. The consequence of this approach is that the alkaline-earth studies were brought to a significantly more advanced state of completion than was the case for iron.

With the preceding paragraph in mind, brief mention concerning the organization of this report is appropriate. Most of the discussion of the alkaline-earth measurements is to be found in Appendices I and II, which are two papers recently submitted (almost simultaneous with this report) for journal publication. The related section in the main body of this report contains a synopsis of Appendices I and II and some valuable ancillary material. This organization of the alkaline-earth material reflects the completed nature of the work, and the author's conviction that the organizational style does not impede understanding of the narration. All the iron results are described in the main body of the report with one exception. The prevaporized liquid-fueled burner used for ferrocene additive measurements was developed under UTC sponsorship, and a description of it is given in Appendix III.

## ALKALINE-EARTH MEASUREMENTS

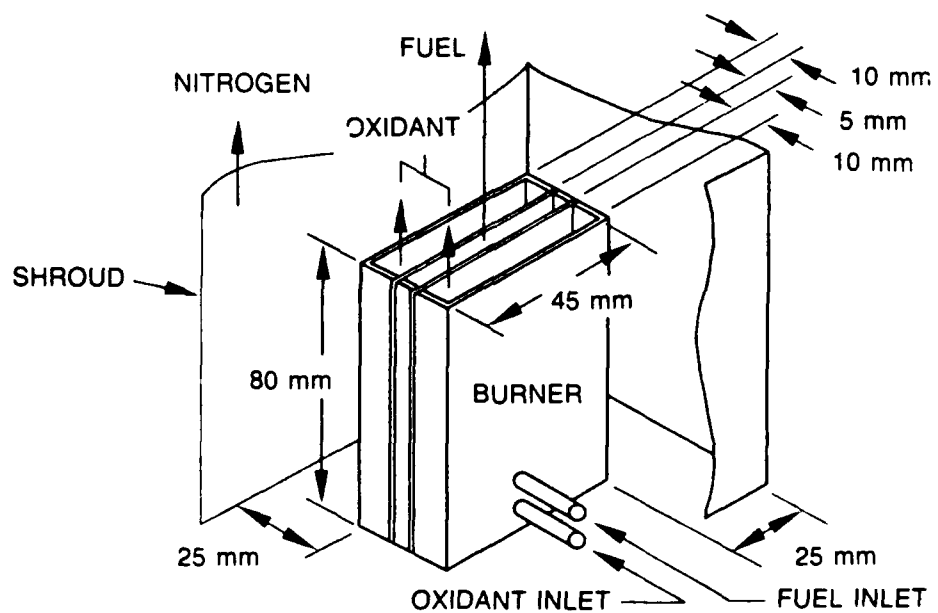
This section contains a synopsis of the measurements which were carried out to determine the effects of alkaline-earth salt additives on soot in a diffusion flame. A detailed discussion of these results is given in Appendices I and II of this report. This synopsis contains some ancillary, but not insignificant data which have not been included in the latter appendices.

The alkaline-earth measurements were made in a laminar, nearly two-dimensional diffusion flame. A diffusion flame was selected in preference to a premixed one since the former soots readily over a wide range of operation, is inherently more stable, and more closely approximates practical combustion media, all of which are diffusion in nature. In addition, the alkaline-earths had been studied previously, in reasonable detail, in premixed ethylene flames (Ref. 2), but not with comparable care and accuracy in a diffusion flame.

The burner which was used to form the preceding diffusion flame is shown schematically in Figure 1 (Refs. 6-9). It is a "symmetric" diffusion flame burner in that the fuel slot has two, and not one, adjacent oxidant slots, which correspondingly causes two separate flame sheets to be formed. In previous work (Refs. 8, 9), the symmetric burner was found to produce a more stable flame than possible with earlier, single oxidant slot versions of it (Refs. 6, 7); consequently, the symmetric burner was used in the work reported here as well. All measurements were carried out with ethylene as the fuel, air as the oxidant, and air as well for the shroud flow, not nitrogen as indicated in Figure 1. The gas flow rates to the burner were such that the flame was highly overventilated causing the two flame sheets to fold inward and form a common apex. In addition, the flame was highly luminous, characteristic of intense soot formation, but there was no visible emission

**SYMMETRIC DIFFUSION FLAME BURNER**

[WOLFHARD, H.G. AND PARKER, W.G., PROC. PHYS. SOC. A62, 722 (1949)]



of soot from its tip; hence, the flame was operated below its smoke point. A photograph of this nearly two-dimensional flame is shown in Figure 1/Appendix II of this report.

Additives were introduced into the flame by pneumatically aspirating aqueous solutions of metallic salts into the oxidizing air stream using a nebulizer taken from a conventional, commercial type (Varian) atomic absorption spectrophotometer. For the particular gas flow rates which sustain the flame, it may be shown that additive insertion as described is the only possible procedure, and this would be just as true were an ultrasonic, as opposed to pneumatic, atomization procedure to be used (Refs. 10, 11). As it turns out, additive introduction into either the fuel or the air (oxidant) streams is equivalent provided that molecular diffusion transverse to the direction of gas flow is sufficiently rapid to bring about uniform additive dispersal. In the discussion which follows immediately below, this was indeed verified to be the case.

In order to verify uniform lateral dispersal of the seeded metals, a sodium additive was selected for the following reason. When NaCl is introduced into a flame, the resulting thermochemistry is relatively simple since species formation is described approximately by (Ref. 12)

$$\text{Na} + \text{X} \rightleftharpoons \text{Na}^+ + \text{e}^- + \text{X},$$

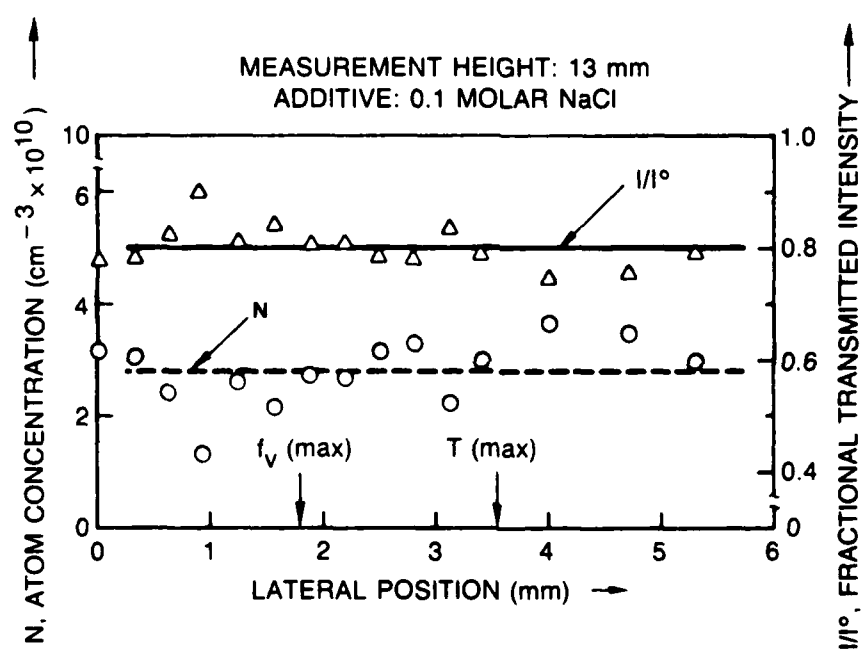
where X is dominant foreign gas collision partner such as, for example,  $\text{N}_2$ . The significance of this reaction is that the number of Na atoms so formed has little or no lateral position dependence in the flame; hence, any variation in Na concentration, measured laterally in the flame, would be evidence of nonuniform seeding of the metals. Na-atom concentrations were determined in a lateral direction and at fixed height by measuring the absorption of laser light at 5890 Å, which corresponds to the atom's  $3s(^2S_{1/2}) \rightarrow 3p(^2P_{3/2})$  transition. The results of these measurements at 13 mm

height are shown in Figure 2, wherein uniform lateral Na-atom dispersal is apparent. The  $I$  and  $I^0$  in Figure 2 are the laser transmitted and incident intensities, respectively. The aspiration rate of the NaCl was much smaller than for the normal additive measurements described in Appendix I. This was done in order to keep the atom concentration sufficiently low and, thereby, assure the occurrence of small absorption values or, equivalently, an optically thin flame. Similar data to those in Figure 2 were obtained at 8 mm height as well.

The rapid molecular diffusion which is evident in Figure 2 may be shown to be consistent with numerical estimates of the diffusivity. The diffusion of atoms from a point source in a laminar flame is given by (Ref. 13),  $N(x,t) = \text{const.} \times \exp(-x^2/4Dt)$ , where  $N(x,t)$  is the number density of species which have diffused the lateral distance,  $x$ , in time,  $t$ , and  $D$  is the diffusion constant in  $\text{cm}^2/\text{sec}$ . For very rapid diffusion, i.e.  $D$  large,  $N(x,t) \rightarrow \text{const.}$ , whereas for very slow diffusion, i.e.  $D$  small,  $N(x,t) \rightarrow 0$ . Using the numerical values  $x = 2.5$  mm and  $D = 9.9$   $\text{cm}^2/\text{sec}$  (for Na) (Ref. 13, Table X.1 therein), as well as residence times,  $t$ , estimated from previous velocity measurements in a flame very similar to that described here (Ref. 9), it may be shown that  $\exp(-x^2/4Dt) \sim 1$  for  $z = 8, 13, 18$  and  $23$  mm. Accordingly, the data in Figure 2 are indeed consistent with numerical diffusivity estimates.

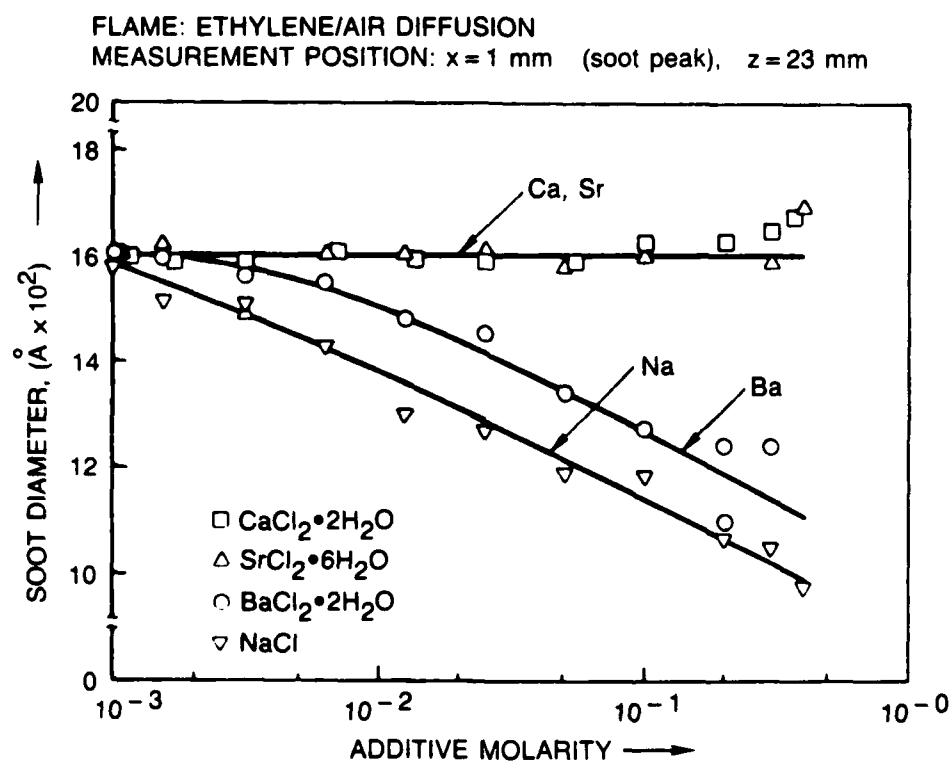
Soot particulates were characterized throughout the flame, with and without additives present, using spatially precise Mie scattering techniques (Refs. 3, 14). Soot diameter,  $D$ , was inferred from the  $20/160^\circ$  angular dissymmetry of scattered laser light, the number density,  $N$ , from the absolute scattered light intensity at one angle, and the volume fraction,  $f_v$ , from the calculated product,  $f_v = (\pi D^3/6)N$ . Representative data of this type for alkaline-earth and Na metal additives are given in Figures 3 and 4. The data

## LATERAL VARIATION OF SODIUM ATOM CONCENTRATION

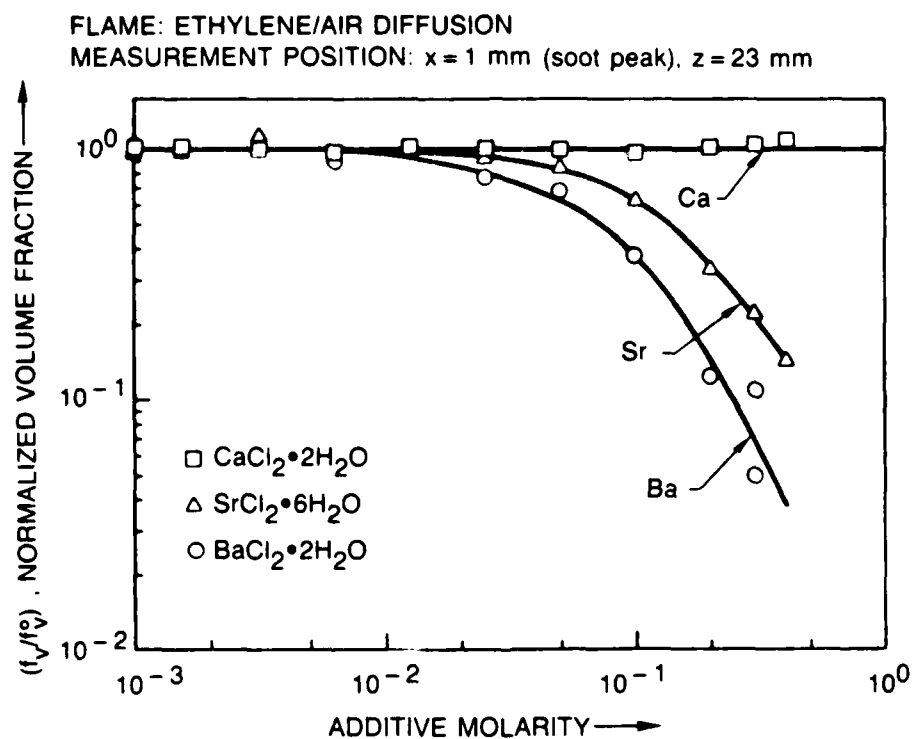




## SOOT SIZE DEPENDENCE ON ADDITIVE CONCENTRATION



## SOOT VOLUME FRACTION DEPENDENCE ON ADDITIVE CONCENTRATION

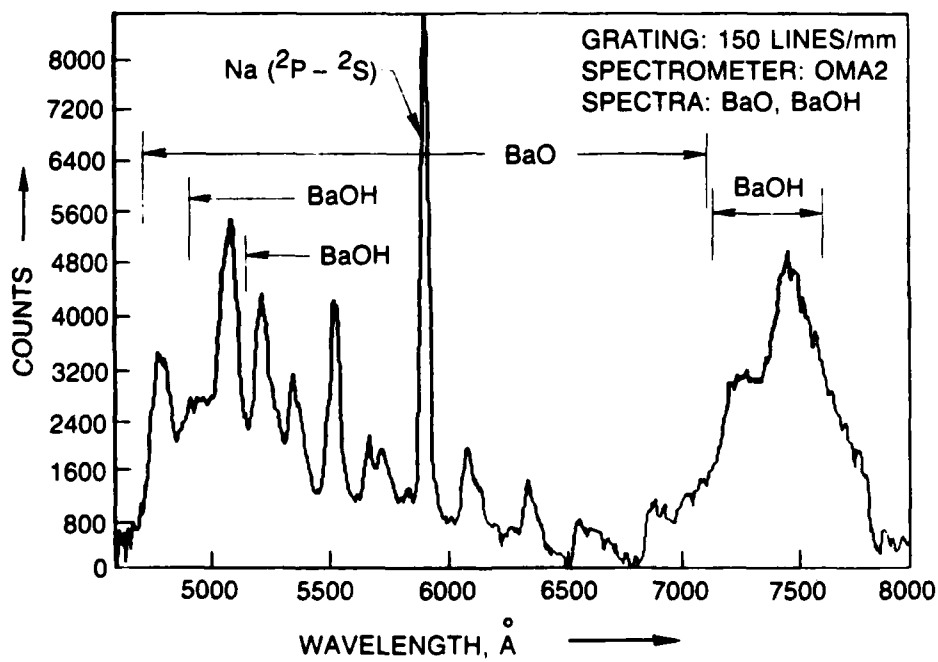


are for a single measurement point in the flame, which is located vertically at 23 mm height and laterally near the flame periphery in the vicinity of the main reaction zone. At this point, the soot loading (or volume fraction) is about equal to its peak value in the flame and, hence, the light scattered from the particulates is intense and readily measurable. The Na measurement was made for comparison with earlier alkali metal data (Ref. 4). For reference, a 0.2 molar solution is equivalent to an approximately 0.2 ppm total metal concentration in the 2000°K flame. In Figure 4, the soot suppression is expressed as  $f_v/f_v^\circ$ , where  $f_v$  and  $f_v^\circ$  are, respectively, the soot volume fractions with an additive salt in solution and with water alone. The data demonstrate that the alkaline-earths alter both  $D$  and  $f_v$  in the order  $Ba > Sr > Ca$ . Note that strontium suppresses soot significantly without experiencing a correspondingly observable size change. (By increasing the strontium aspiration rate, a roughly 10% decrease in size can be observed at  $x = 1$ ,  $z = 23$  mm for a 0.2 molar  $SrCl_2 \cdot 6H_2O$  solution. This is apparent in Table I and Figure 4a/Appendix I.) In this case, then, the reduction in  $f_v^\circ$  is brought about almost entirely by an accompanying decrease in  $N^\circ$ . This suggests that it is not adequate to regard the metal cation as merely acting to inhibit agglomerative soot growth, as is more likely the case for alkali metals, but rather to view Sr as perturbing earlier combustion stages. This view is not inconsistent with the Ba data in Figures 3, 4. Owing to a lower ionization potential (Ref. 15), barium produces a significantly higher concentration of  $MOH^+$  ( $M = Ba, Sr$ ) than does strontium and, hence, a decrease in  $D$  is apparent. However, as is evident in Figure 3 this decrease is greater for sodium, which produces significantly fewer cations than does barium, an observation also not consistent with simple agglomerative interruption.

The effect of additives on soot was measured at locations other than that appropriate to Figures 3 and 4. These data may be found in Figures 4, 5 and 6/Appendix I. There it is apparent that additive effectiveness is very position dependent, and that the  $Ba > Sr > Ca$  order of effectiveness is preserved at all positions. It is reasonably accurate to conclude from these data that the alkaline-earth metals are most effective in the vicinity of temperature maxima or the main reaction zone of the flame, which not coincidentally, as discussed in detail in Appendix I, is where flame radicals and metal cations are primarily present.

In order to formulate a chemical/kinetic description of additive behavior in relation to soot suppression, it is necessary, at the very least, to understand the details of metal combustion in the flame. For example, if the species so formed are identified and their concentrations reliably measured, then suppression may be related to one or more of the latter species. The combustion of alkaline-earth metals is relatively complex, but fortunately reasonably well understood (Ref. 16). In fact, it is known that the species  $M$ ,  $MO$ ,  $MOH$ ,  $M(OH)_2$ ,  $M^+$  and  $MOH^+$  ( $M = Ca, Sr, Ba$ ) are formed and, moreover, numerical values are available for the equilibrium constants appropriate to the several reactions which describe metal/radical (flame) interaction. Species were identified in this work from optical emission measurements. One such example is given in Figure 5 wherein low resolution  $BaO$  and  $BaOH$  spectra have been identified. Similar data, at higher resolution, are given in Figure 7/Appendix I for the  $5300 < \lambda < 6100 \text{ \AA}$  wavelength interval. Therein the existence of  $Ba$  in the flame is confirmed, and more accurate  $BaO$  spectral signatures are present. As in Figure 5, the  $Na$ -atom emission line is due to a very low level impurity and, hence, has no bearing on data interpretation.

## BARIUM SEEDED ETHYLENE/AIR FLAME SPECTRA



Of the six species above, the four neutral entities were observed via optical emission; but for reasons discussed in Appendix I the two cations were not observed directly and, thus, it was necessary to assume their presence.

Initially, an attempt was made to measure the species concentrations via saturated laser-induced fluorescence. This approach, however, was not successful for reasons discussed at length in Appendix I. Instead, the concentrations were estimated from the equilibrium constants mentioned above, and measured values of  $[H]/[H_2O]$  required for this approximate semi-empirical approach. In order to test the accuracy of this procedure, direct measurements of  $[Ba]$ ,  $[Sr]$  and  $[Ca]$  were made via optical absorption. Satisfactorily the  $[M]$  concentrations from optical absorption were in reasonable agreement with values obtained from the reaction equilibrium constants, thereby verifying the essential correctness of the latter procedure.

Results for the metal species concentrations demonstrated that only for  $[MO]$  and  $[MOH^+]$  were the relative Ca/Sr/Ba numerical values suggestive of a  $Ba > Sr > Ca$  order of soot removal. Thermodynamic arguments were used to rule out the significance of  $[MO]$ . In support of this conclusion, measurements were made of the effect of a 0.2 molar  $SnCl_2 \cdot 2H_2O$  additive on soot in the diffusion flame, and the additive was observed to be totally ineffective despite the fact that its known thermochemistry indicates that  $SnO$  is by far the preponderant combustion product. Based on this and similar reasoning,  $[MOH^+]$  was concluded to be the critical species. The reason for this is that:

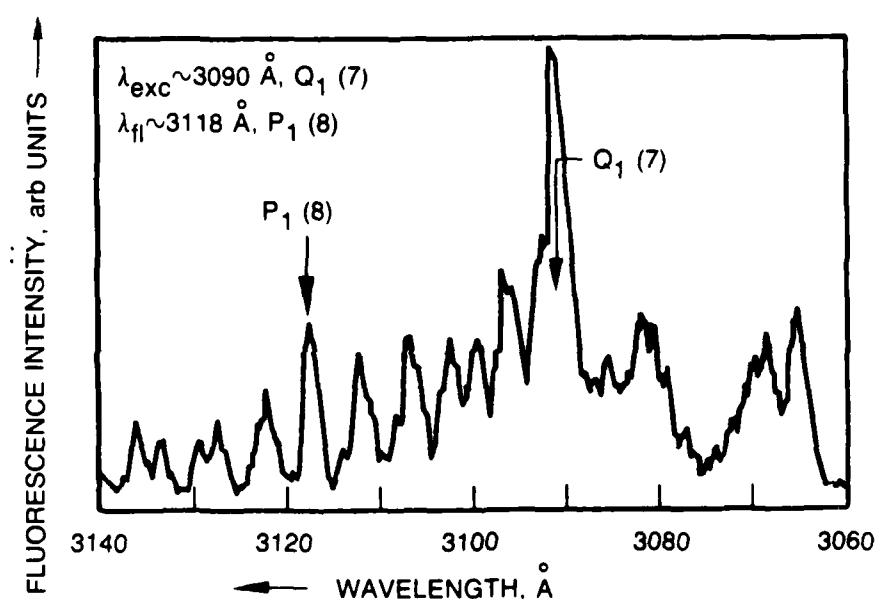
- 1) as mentioned, the relative values of  $[MOH^+]$  for Ca, Sr and Ba are suggestive of the relative soot removal efficiencies of the latter metals;
- 2) since the rate of ion production,  $d[MOH^+]/dt$  is proportional to  $[H]^3$ , it has a very pronounced lateral dependence in agreement with that for additive

effectiveness; 3) results for various metal additives given in Table V/Appendix I show an excellent correlation between ionization potential, or number of metal cations, and soot suppression.

The preceding discussion is suggestive of an electrical mechanism of soot removal; however, there have been repeated speculations in the published literature concerning a possible chemical/OH explanation of alkaline-earth metal behavior in relation to soot suppression (Refs. 17-19). The reduction is presumed to occur as follows. In a flame under equilibrium conditions, the OH concentration is determined by the balanced reaction,  $\text{OH} + \text{H}_2 \rightleftharpoons \text{H}_2\text{O} + \text{H}$ . If soot is present, accompanied by intense OH oxidation of it, then the OH concentration in the balanced reaction may, in fact, be below its equilibrium value. When a metal atom is introduced into the flame, it may catalyze an increase in [H] via  $\text{M} + \text{H}_2\text{O} \rightarrow \text{MOH} + \text{H}$ , or  $\text{M} + 2\text{H}_2\text{O} \rightarrow \text{M}(\text{OH})_2 + 2\text{H}$ . This, then, has the effect of driving the balanced reaction to the left, thereby increasing the [OH], which results in accelerating soot oxidative removal via  $\text{C}(\text{solid}) + \text{OH} \rightarrow \text{CO} + (1/2)\text{H}_2$ . The first quantitative test of this mechanism was carried out during the course of this contract; a detailed discussion of it is given in Appendix II. Here the results are briefly summarized and some supplementary data are presented.

In order to test the OH mechanism, hydroxyl radical concentrations are required. The OH concentrations were inferred from saturated laser-induced fluorescence measurements, using exciting light near 3090 Å, obtained by frequency doubling the output of a pulsed, visible dye laser. The observed laser-excited fluorescence spectrum of OH is shown in Figure 6. The data are for  $Q_1(7)$  excitation at  $\lambda \sim 3090$  Å. The spectral resolution is sufficiently high to resolve some individual rotational transitions such as  $P_1(8)$  and its immediate, neighboring transitions. To determine OH concentrations, the

## LASER EXCITED OH FLUORESCENCE SPECTRUM



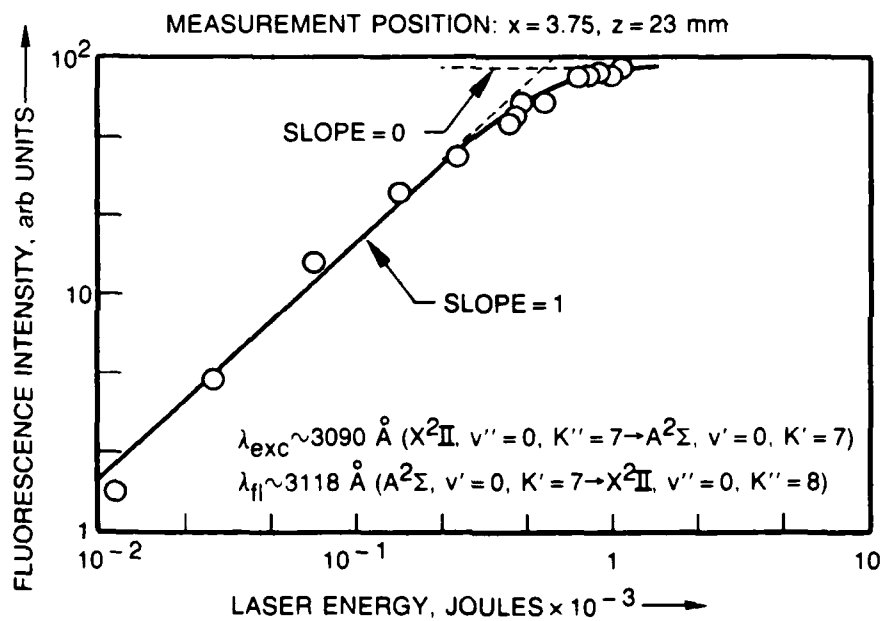


radicals were excited at  $Q_1(7)$  and fluorescence was observed only at  $P_1(8)$  with the aid of a spectrometer. The  $P_1(8)$  fluorescence as a function of laser energy is shown in Figure 7. Near complete saturation of fluorescence is evident at  $1 \times 10^{-3}$  Joules laser energy for a  $x = 3.75$  mm lateral position. Saturation was observed at other lateral positions as well and, hence, OH concentrations were measured laterally across the full width of the luminous zone of the flame; these data are shown in Figure 4a/Appendix II. The position of the peak OH concentration without an additive present,  $N_{OH}^{\circ}(\max)$ , is shown in Figure 8 in relation to the temperature profile at 23 mm height and the position of the soot peak,  $f_v(\max)$ . In order to test the hypothesis of metal-induced [OH] increase, the latter concentration was measured without and with a  $BaCl_2 \cdot 2H_2O$  additive. Figure 9 shows clearly that the additive decreases [OH], and not the reverse as speculated upon earlier by others (Refs. 17-19). Other data which may be found in Appendix II demonstrate that this conclusion applies to positions in the flame other than those given in Figure 9 and to Ca and Sr metal additives as well. Accordingly, the results reported here do not support the chemical/OH mechanism as a viable explanation of alkaline-earth behavior.

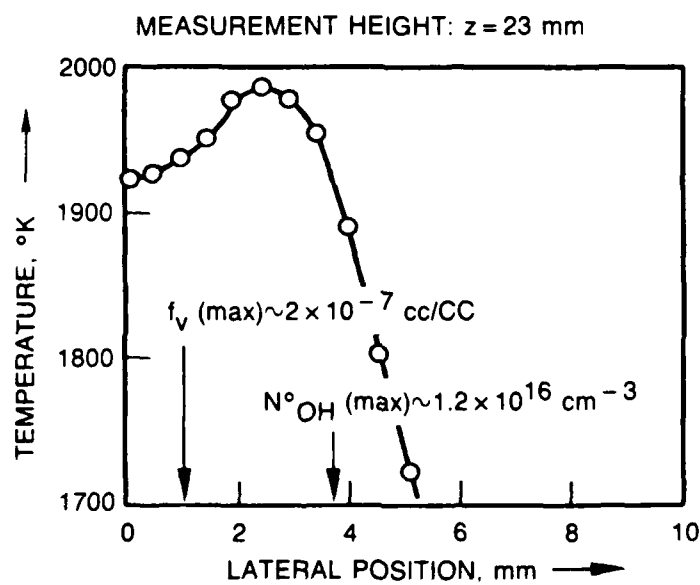
The most significant conclusions of the alkaline-earth and related metal additives measurements described in this report are as follows:

- 1) The alkaline-earth metals act to suppress soot in the order  $Ba > Sr > Ca$ .
- 2) Although the metals perturb both soot diameter,  $D$ , and number density,  $N$ , suppression is due principally to a decrease in  $N$ .
- 3) The data suggest additive intervention at more than just the agglomerative soot formation stage.

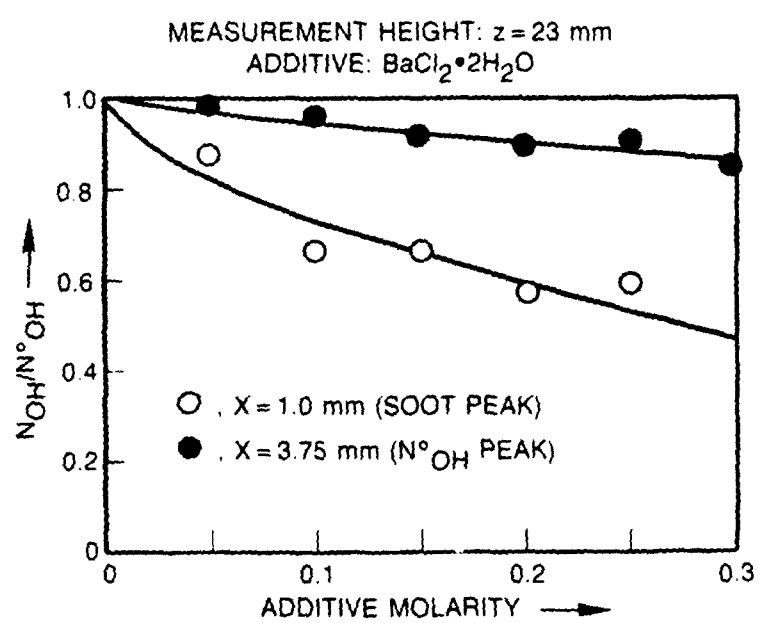
## SATURATED LASER EXCITED OH FLUORESCENCE



## LATERAL DEPENDENCE OF FLAME TEMPERATURE



## BARIUM SUPPRESSION OF OH CONCENTRATION



- 4) Additive effectiveness varies with measurement position in the flame, increasing or decreasing in direct relation to the local temperature.
- 5) Charged as opposed to neutral metal species are responsible for soot suppression; the degree of suppression and a metal's ionization potential are very strongly correlated.
- 6) For alkaline-earths, the  $\text{MOH}^+$  ( $\text{M} = \text{Ba}, \text{Sr}, \text{Ca}$ ) are critical to soot removal.
- 7) Metal-induced enhanced oxidation of soot by OH is not a correct explanation of alkaline-earth behavior as concerns soot suppression.

## IRON MEASUREMENTS

This section describes measurements which were carried out to determine the behavior of iron compounds as fuel additives. Unfortunately, this research is not as complete as that for the alkaline-earths, due about equally to difficulties which were encountered and to the unexpectedly large fraction of the contract period which was necessary in order to achieve a reasonably complete quantitative description of alkaline-earth fuel additive properties. Nevertheless, a significant quantity of useful iron data were obtained, and are presented here. Several different fuel/additive/burner configurations were studied, and the discussion below is segregated accordingly.

## WOLFARD-PARKER FLAME

Iron additive measurements were made for the same  $C_2H_4$ /air diffusion flame used for the alkaline-earths and described above and in Appendix I. Representative results which give the effect of iron on soot size, number density and volume fraction are shown in Table I. Measurements were

TABLE I. SPATIAL DEPENDENCE OF ADDITIVE EFFECTIVENESS FOR A 0.2 MOLAR  $Fe(NO_3)_3 \cdot 9H_2O$  ADDITIVE

z →	Measurement height, mm				
	13	18	23	28	38
D, Å	1136	1141	1538	1655	1579
D/D°	1.07	1.02	1.01	1.02	1.03
N/N°	0.78	0.98	1.07	1.17	1.61
$f_v/f_v^\circ$	0.97	1.05	1.10	1.23	1.76

made at five different positions. The vertical coordinates were those indicated in Table I. In each case, the horizontal coordinate was located just inside the flame periphery and coincident with the position corresponding to the peak soot volume fraction. As such, then, the data in Table I are for different vertical positions along and very near the main reaction zone. The significance of this data is that unlike the alkaline-earths the iron salts cause an apparent increase in the quantity of soot initially present. This is particularly true at  $z = 28$  and  $38$  mm since for these data the increase exceeds measurement error; conversely, the  $N/N^\circ$  and  $f_v/f_v^\circ$  decreases at  $z = 13$  mm are within error and, hence, a conclusion concerning their validity is not possible. The alteration of soot diameter, if any, is very small; hence, as for Sr, for example, the change in volume fraction is caused principally by an increase in number density. It should be noted, however, that if the additive aspiration rate is increased strongly, it is possible to observe an increase in both  $D^\circ$  and  $N^\circ$ . For example, under conditions of very heavy seeding at  $z = 23$  mm with  $\text{Fe}(\text{NO}_3)_3$ , the soot parameter changes were  $D/D^\circ = 1.19$ ,  $N/N^\circ = 3.30$ , and  $f_v/f_v^\circ = 5.61$ . Finally, it may be worth noting that in addition to the soot increase observed for  $\text{Fe}(\text{NO}_3)_3$ , similar data were obtained for  $\text{FeSO}_4$ ,  $\text{Mn}(\text{NO}_3)_2$  and for 1, 1' - ferrocene dicarboxylic acid in 14%  $\text{NH}_4\text{OH}$  (ferrocene = dicyclopentadienyl iron).

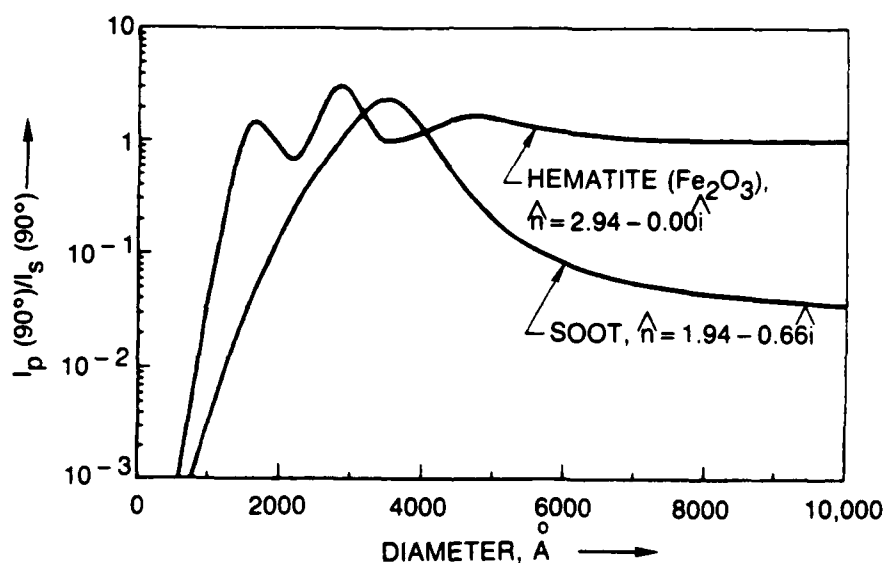
In the discussion above, the observed increase in particulate loading was assumed to be due to an increase in soot formation. In principle, however, this conclusion should be made cautiously since it is possible, under certain conditions, for solid metal oxide particles to form in an iron seeded flame. These particles may, then, scatter light in a manner indistinguishable (possibly) from that for soot. In a flame, the condition favorable to particle formation may be considered to occur when the partial pressure of the

total metal species concentration approaches or exceeds the vapor pressure above the solid metal oxide. In this regard, flames to which Ba and Fe salts are added behave quite differently. Typically, the metal species concentration in a Ba seeded flame is approximately  $10^{13}/\text{cm}^3$  for a 0.5 molar or so nebulized solution. At 2000°K, this corresponds to about a 2 mTorr metal partial pressure. On the other hand, the vapor pressure above BaO at 2000°K is approximately 100 mTorr; consequently, particle formation is unlikely. Omitting further details, it may be shown that for a similar 2 mTorr Fe metal pressure the chances for particle formation are much more favorable since, at 2000°K, the vapor pressure above solid FeO is about 6 mTorr. Further, it may be shown that at somewhat lower temperatures the probability of particle formation increases. Clearly, then, there is indeed a significant distinction between Ba and Fe as regards their tendencies to form solid oxides. Unfortunately, sufficient information was not available to estimate the probability of solid ( $\text{Fe}_x\text{O}_y$ ) formation in our flame.

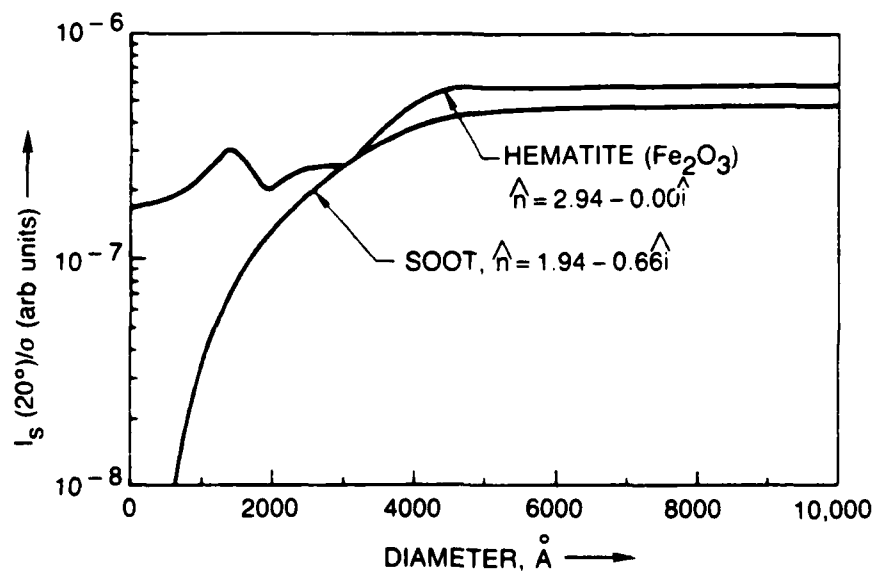
Fortunately, there is a way to cope with the preceding difficulty and, thereby, discriminate between the metal oxide and soot. The solution is to exploit the small but different optical behaviors of the two chemically dissimilar particulates. One example of their optical dissimilarity is given in Figure 10, wherein the polarization dependence of light scattering at 90° is seen to differ for hematite and soot. Along similar lines, it is apparent in Figure 11 that the ratio of scattering at 20° to extinction also differs for the two solids, and that the dissimilarities in Figures 10 and 11 are not equivalent. In order to search for metal oxide formation, measurements of the preceding type were made in the ethylene/air flame and are summarized in Figure 12. There the two ratios, both of which are in principle strongly size dependent, are seen to be insensitive to increasing  $\text{Fe}(\text{NO}_3)_3$  addition, and may



## LIGHT POLARIZATION DEPENDENCE ON PARTICULATE SIZE



## LIGHT SCATTERING/EXTINCTION RATIO DEPENDENCE ON PARTICULATE SIZE

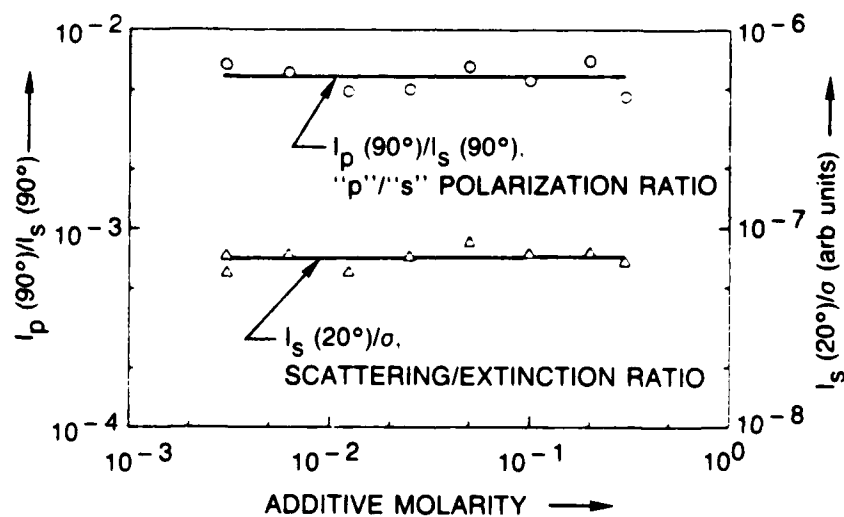


# SIZE DEPENDENT LIGHT INTENSITY RATIOS VS ADDITIVE CONCENTRATION

FLAME: ETHYLENE/AIR DIFFUSION

MEASUREMENT POSITION:  $x = 1$  mm (soot peak),  $z = 23$  mm

ADDITIVE:  $\text{Fe}(\text{NO}_3)_3 \cdot 9\text{H}_2\text{O}$



be shown to yield an invariant 1500 to 1600 Å particulate diameter characteristic of the unseeded flame soot. Since both ratios yield the same size and are both insensitive to additive molarity, solid ( $\text{Fe}_x\text{O}_y$ ) formation is ruled out, at least for volume fractions comparable to or exceeding those for soot. Accordingly, then, the observed increase in particulate loading in the presence of  $\text{Fe}(\text{NO}_3)_3$  is indeed due to soot and not metal oxide formation.

Finally, and parenthetically, it should be mentioned that soot enhancement has been observed recently for a premixed ethylene flame seeded with ferrocene (Ref. 20), and a detailed explanation has been developed for this enhancement. (The author of this report regards it as improper for him to discuss these as yet unpublished results here; the interested reader is encouraged to contact Prof. Adel F. Sarofim of the Massachusetts Institute of Technology for details.)

#### WICK FLAME

Measurements were made to determine the effectiveness of organometallic iron compounds as soot suppressants in flames derived from liquid fuels having a significant aromatic content. Primary emphasis was given to ferrocene since it is an additive which has significant practical importance. For example, ferrocene has been observed to inhibit sooting in: jet and domestic burners; flow reactor acetylene pyrolysis (Ref. 21); diesel combustion of petroleum hydrocarbons (Refs. 22, 23); aircraft and utility gas turbine engines (Ref. 24); poly (vinyl chloride) combustion (Ref. 25).

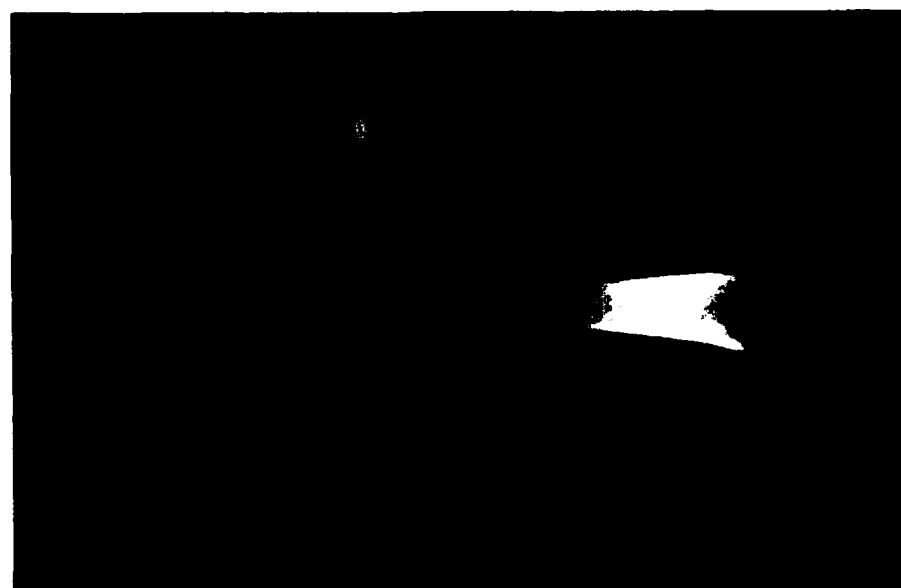
Initially, ferrocene measurements were done with a wick flame. The burner, in this case, was exceedingly simple in design. A small bottle, having a roughly 50 ml capacity, was filled with liquid fuel, a wick was passed through a narrow opening in the bottle cap, and the evaporating fuel

was then ignited. For this wick flame, the sooting which occurred for a 5/1 iso-octane/ toluene fuel mixture without additives present was compared with the case in which ferrocene was added to the fuel in varying, small concentration. For 0.25% ferrocene by weight, a heavy soot plume was suppressed as determined by visual observation. A photograph of this result is shown in Figure 13. In order to make this test more quantitative, optical extinction measurements were made at different heights in the flame. The light extinction decreased in the presence of ferrocene, albeit differently for different points in the flame, thereby confirming and extending the visual observation of soot suppression. Attempts were made to evaluate other substances closely related to ferrocene, but these were either not successful or resulted in soot suppressions less pronounced than for ferrocene itself. For example, 1,1'-ferrocene dicarboxylic acid was insoluble in the above fuel mixture, and hydroxymethyl ferrocene, although soluble, was significantly less effective than ferrocene. Specifically, the effects of 150 mg of additive in a 30 ml fuel mixture were compared for ferrocene,  $(C_5H_5)_2Fe$ , and hydroxymethyl ferrocene,  $HOCH_2C_5H_4FeC_5H_5$ , both of which are inert solids. Without an additive a heavy soot plume was present; with ferrocene the plume disappeared completely, whereas with hydroxymethyl ferrocene a light to medium soot plume remained. The reason for this unequal behavior remains unclear; the difference may be due to more rapid evaporation of the ferrocene from the hot surface of the wick, but there is no easy or clear way to test this conjecture.

The wick flame measurements were valuable in that the significance of ferrocene as a soot suppressant was made very evident. The difficulty with a burner of this type is, however, that fundamental combustion parameters such as fuel and additive type, fuel flow rate and additive concentration,

SOOT REDUCTION WITH FUEL ADDITIVE FOR WICK FLAME

FLAME: DIFFUSION/WICK  
FUEL: ISO-OCTANE/TOLUENE MIXTURE  
ADDITIVE: FERROCENE



a) NO ADDITIVE



b) 0.25% FERROCENE

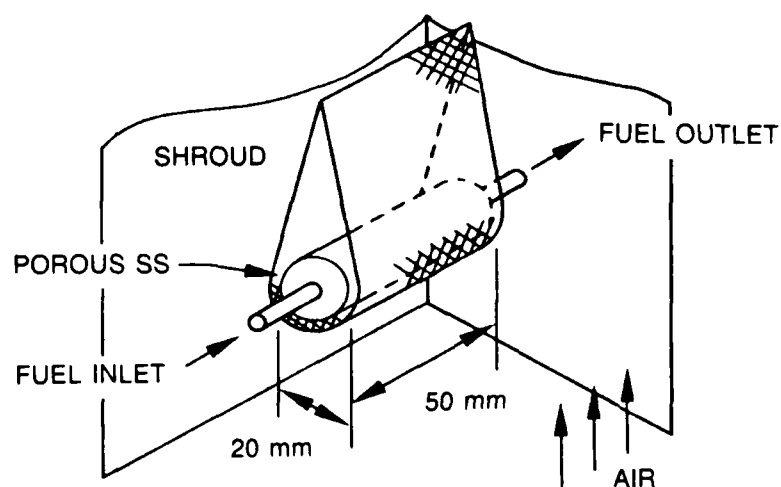
and flame temperature are not easily varied. For these reasons, the wick approach was dropped in favor of the porous cylinder diffusion flame which is described immediately below.

#### POROUS CYLINDER FLAME

An attempt was made to make ferrocene measurements in a liquid counterflow diffusion flame using a porous cylinder burner patterned closely after one described by Abdel-Khalik et al. (Ref. 26). This flame is shown schematically in Figure 14. For it, fuel penetrated to and evaporated from the outer surface of a porous cylindrical shell. There the fuel was ignited in the presence of flowing shroud air creating a reasonably well-defined diffusion flame. The flame was laminar at and near the forward stagnation zone of the fuel/air counterflow but became increasingly turbulent higher up in the flame. The several mm thick forward stagnation zone is located near and under the lower cylinder surface in Figure 14; turbulence higher in the flame is not shown. In order to evaluate ferrocene effectiveness in this case, optical extinction measurements were made in the laminar zone for a fuel mixture and ferrocene concentration similar to the above wick flame case; the latter zone alone lends itself to optical probing. These measurements did not yield any demonstrable ferrocene effectiveness. In order to verify that ferrocene or its derivatives were indeed present in the flame, particulate samples were collected in the postflame zone and analyzed for Fe presence by SIMS (secondary ion mass spectrometry). In this way, Fe was detected leading to two indistinguishable conclusions. The first is that additive effectiveness, if present, occurs for long residence times in turbulent zones not readily amenable to optical extinction or scattering measurement. The second is that the cool cylinder surface, relative to the wick, hinders

**POROUS CYLINDER DIFFUSION FLAME**

[ABDEL-KHALIK, S.I., TAMARU, T., AND EL-WAKIL, M.M.,  
15TH SYMPOSIUM (INTL) ON COMBUSTION]





evaporation of ferrocene in sufficient quantity to perturb soot. Unfortunately, neither of the two surface temperatures are readily measurable. In summary, since additive effects could not be observed in the porous cylinder flame, for reasons perhaps not fundamental such as inefficient ferrocene injection, this approach was abandoned in favor of the approach described below.

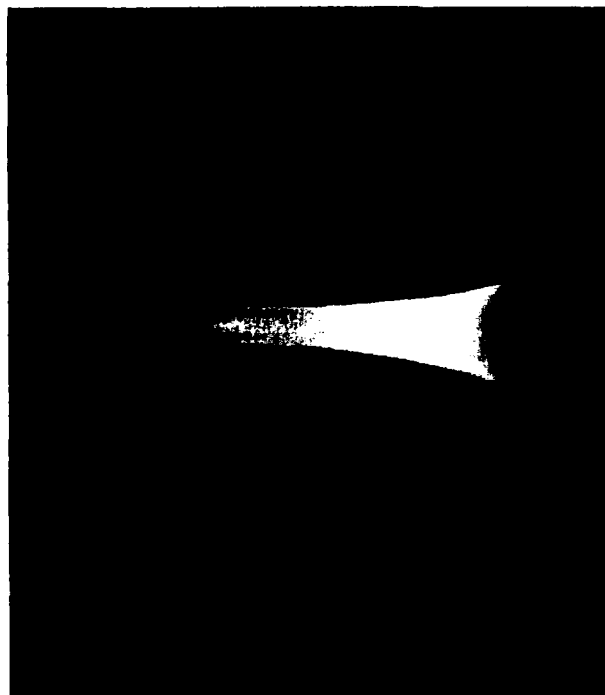
#### PREVAPORIZED LIQUID-FUELED FLAME

While the preceding iron measurements were in progress, a parallel effort took place to develop a much more flexible burner system for ferrocene measurements. This latter effort was supported entirely by the Government Products Division of Pratt and Whitney in West Palm Beach, Florida. A description of the construction of this burner and tests which were conducted to verify its utility for ferrocene studies are described in a report prepared for Pratt and Whitney and reprinted here as Appendix III. A burner identical to that described in Appendix III was used during the course of this AFOSR contract to make Mie scattering measurements of soot from a prevaporized 5/1 iso-octane/toluene flame with and without ferrocene present. These results are discussed directly below.

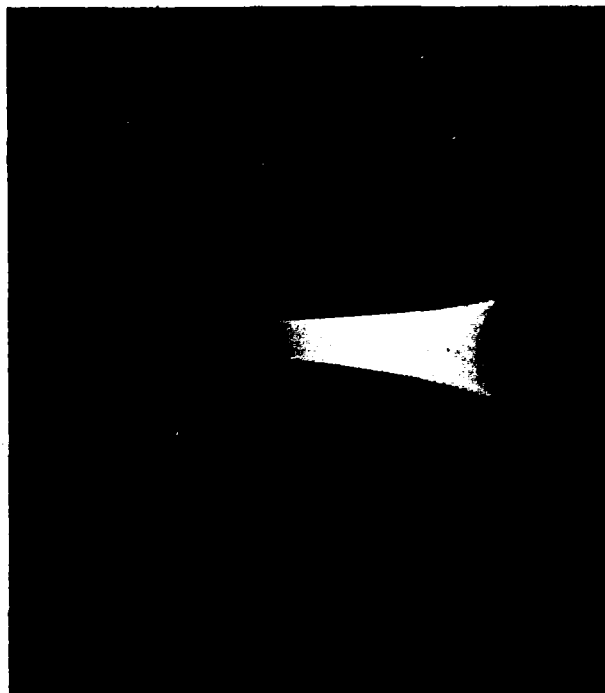
In Figure 15a, there is a photograph of a sooting, axisymmetric diffusion flame emanating from the burner mentioned in the preceding paragraph. The fuel flow rate of 0.1 ml/min is sufficient to cause the flame to operate above its smoke point, thereby creating a clearly observable plume. The threshold for smoke formation for this particular flame is about 0.07 ml/min. The effect of 0.3% (by wgt.) ferrocene fuel additive on this flame is strikingly evident in Figure 15b, where the smoke is seen to be suppressed entirely. In this sense, these data in effect replicate similar data observed with the wick flame and described above.

# SOOT REDUCTION WITH FUEL ADDITIVE FOR PREVAPORIZED LIQUID-FUELED FLAME

FLAME: DIFFUSION/PRE-HEATED FUEL BURNER  
FUEL: 20% TOLUENE/80% ISO-OCTANE MIXTURE  
FUEL FLOWRATE: 100 $\mu$ l/min (POSITIVE DISPLACEMENT PUMP)  
ADDITIVE: FERROCENE



a) NO ADDITIVE

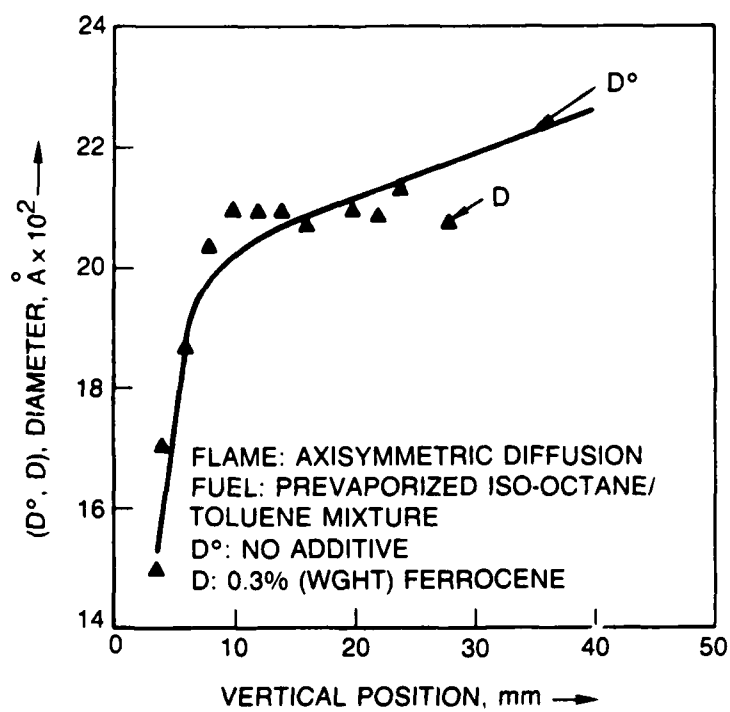


b) 0.3% FERROCENE

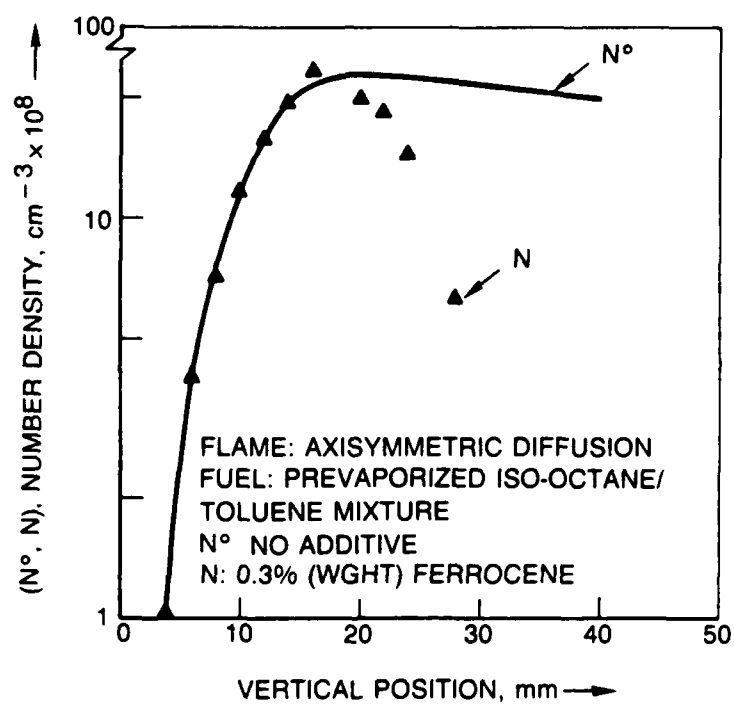
In order to determine more accurately the effect of ferrocene on soot, detailed Mie scattering measurements of soot size, number density and volume fraction were made with and without the additive present. These results are shown in Figures 16, 17 and 18, wherein additive influence on  $D^\circ$ ,  $N^\circ$  and  $f_v^\circ$  has been determined at the burner axis ( $r = 0$  radial distance) for various vertical positions in the flame. The measurements terminate at  $z = 40$  mm with no additive and near  $z = 30$  mm with the additive present. It was not possible to avoid this 10 mm gap since the flame tip flickered significantly with the additive present, which resulted in very unsteady Mie signal intensities. The data show that up to about  $z = 20$  mm the ferrocene does not alter the soot parameters. Beyond this position, however, there is a very pronounced effect on  $N^\circ$  and  $f_v^\circ$ , with a smaller, more questionable decrease present for the diameter,  $D^\circ$ . Since even at  $z = 3$  mm (first data point), the soot particulates are fully formed (but not fully agglomerated), the data indicate that ferrocene acts to suppress soot at a very late combustion stage.

For Ba measurements taken with the Wolfhard-Parker burner, the additive was found to have a very pronounced dependence on lateral position. This was not the case, however, for ferrocene. Figure 19 shows that at  $z = 12$  mm, the additive does not perturb soot at all lateral (or radial) positions, even that near the reaction zone at  $x = -2$  mm.

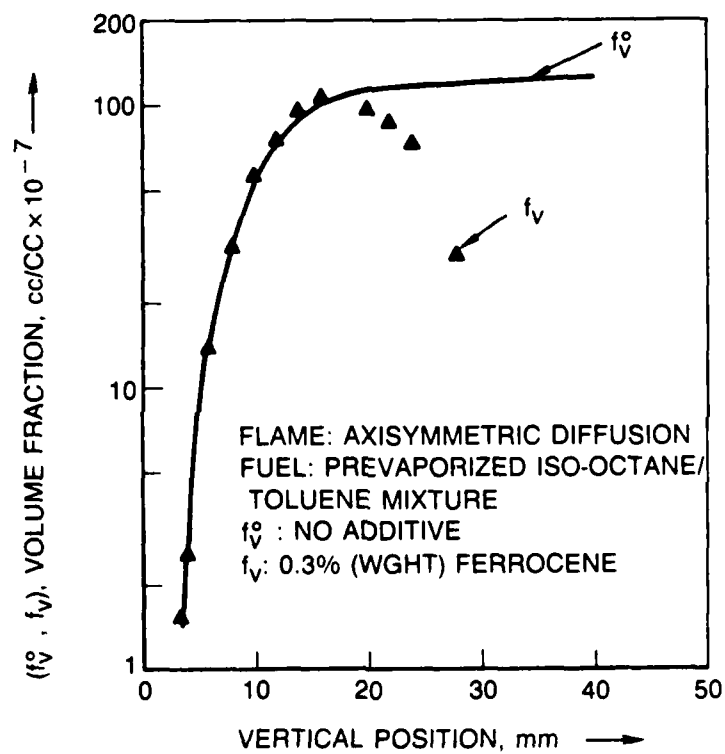
## ADDITIVE EFFECTIVENESS ON DIAMETER



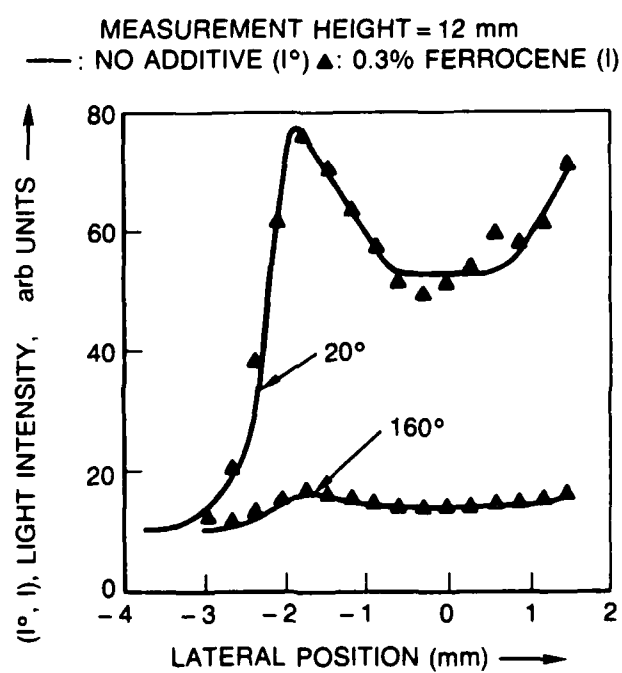
## ADDITIVE EFFECTIVENESS ON NUMBER DENSITY



## ADDITIVE EFFECTIVENESS ON VOLUME FRACTION



## ADDITIVE EFFECTIVENESS ON SCATTERED LIGHT INTENSITY



## DISCUSSION

In this section, a summary is given of the principal achievements of this contract research as well as the areas in which difficulties were encountered. Separate discussion of these details is given for the alkaline-earth and iron metal additives. The section concludes with an outline of future research plans.

## ALKALINE-EARTH ADDITIVES

New and significant results were obtained during the course of this contract research for the alkaline-earth metals as fuel additives. The principal contribution which has been made may be described, in fact, quite simply. For the first time, soot, temperature and metal combustion species have been characterized in-situ and with spatial precision throughout a flame, either premixed or diffusion. In addition, soot suppression has been related to a specific cationic metal combustion product, and the hydroxyl radical mechanism of soot suppression has been discredited. In order to underscore the positive contribution which these results have made, as well as to put them in their proper perspective, a brief encapsulation of selected earlier alkaline-earth measurements is given immediately below.

Earlier, Cotton, Friswell and Jenkins (Ref. 17) made measurements in a propane/oxygen diffusion flame for some forty metal additives, including the alkaline-earths. The amount of soot emitted was determined by weighing the solid material collected on filter paper. This gave no information regarding particulate size and number density with and without additives present. The authors gave an approximate analysis for the alkaline-earth metals, arguing that they catalyze the production of hydroxyl radicals which remove soot via oxidative reactions with solid carbon, a conclusion which our work has shown to be inaccurate. Bulewicz, Evans, and Padley (Ref. 27) observed that



metallic additives may promote as well as inhibit soot depending on the choice of additive and its concentration. They determined that additive cations and not neutral species were responsible for alterations in the quantity of soot present. The soot was characterized by extracting it from the postflame gases with a filter and measuring the particulate size and number density via electron microscopy. Changes in both of these parameters were observed in the presence of additives. Feugier determined the effects of alkali and alkaline-earth metals on the sooting tendency of premixed ethylene/oxygen flames (Ref. 19). In this case, the volume fraction of soot present was determined by measuring the luminous intensity of the flame and comparing it with the intensity of a calibrated source. The soot promoting and inhibiting action of the additives tested in Reference 27 was confirmed by Feugier; however, a different interpretation was given to the inhibiting effect in that hydroxyl radicals were taken as responsible for it, and not ions. A novel aspect of this work was the attempt to differentiate additive effects on the various stages of particulate formation and growth. In this regard, transition metals were determined to be effective principally in the agglomerative stage, whereas barium was found to be effective in earlier stages. Recently, Haynes, et al. (Ref. 2) made measurements similar to those of Reference 19 with respect to the flame and additives; however, the particulate size and number density were determined in-situ from an analysis of Mie scattering of cw laser radiation by the particulates. Unfortunately, there are significant differences in both the observations and interpretations in References 2 and 19. The preceding experiments are inadequate in important respects. Except for Haynes, et al., the particulates are not characterized by in-situ measurement; moreover, in Reference 2, the use of a Rayleigh approximation to the exact, Mie scattering theory is a questionable procedure. None of the experiments above identified the neutral and/or ionic additive species present

in the flame, nor were any spatially precise in-situ measurements of species concentration made. Finally, Howard and Kausch (Ref. 1) pointed out earlier that there are serious discrepancies in the work of Bulewicz, et al. (Ref. 27) and Haynes, et al. (Ref. 2).

The contract research described in this report has been valuable in that an improved understanding of alkaline-earth suppression of soot has been achieved. It is important to point out, however, that a complete understanding is not yet in hand. In this work, an active metal species has been identified, but the exact soot suppressing mechanism has not been established. This will require, at the minimum, data which convincingly establish the stage(s) at which the additive intervenes, and an optical or other means of probing the  $\text{MOH}^+$  directly would also be helpful. Future research plans to meet these objectives are outlined below.

#### IRON ADDITIVES

The principal contribution in the area of iron additives has been to map their behavior on soot size, number density and volume fraction throughout a flame, a measurement not previously made. In so doing, iron has been observed to suppress soot, but also to promote its formation under certain circumstances. The principal deficiency in this work is that the active iron combustion species has not been identified, which will be the priority of future work. Since the ionization potential of iron is 16.18 eV as opposed to 4.35 eV for  $\text{BaOH}^+$ , it is not anticipated that ions are responsible for either soot inhibition or promotion in flames seeded with iron additives. As such, the relevant mechanisms for Ba and Fe seeding may be distinctly dissimilar.

#### FUTURE RESEARCH PLANS

Work on alkaline-earth and related fuel additives will continue at UTRC under AFOSR Contract No. F49620-86-C-0054. This research will attempt to deal

successfully with the issues raised above. For it, use will be made of both optical and mass spectrometric techniques to measure the effects of selected fuel additives on soot in premixed flames. For species determination, optical methods will remain the first choice due to their in-situ and spatially precise nature, but as pointed out above there are instances where laser/optical approaches are not applicable. In such cases, recourse will be made to mass spectrometry as a necessary and highly useful alternative. For example, laser/optical techniques will be used to characterize particulate parameters down to approximately  $(10-30) \text{ \AA}$  in size, to measure concentrations of additive species with known spectra, and finally where applicable to measure concentrations of significant unseeded flame species like, e.g., the hydroxyl radical. Mass spectrometry, on the other hand, will be used to probe important species without known optical spectra, such as soot precursors and intermediates as well as additive species. Measurements will be carried out to determine the effects of additives on various stages of soot formation, with attention given to parameters such as fuel and additive type, equivalence ratio and temperature. The approach will emphasize premixed as opposed to diffusion flames. The former lend themselves more readily to analytical study as, for example and significantly, in the calculation of ambient and seeded species concentrations. Secondly, soot formation and burnout are more readily kept separate in premixed than in diffusion flames, which simplifies the kinetic analysis. For fundamental reasons and to facilitate mass spectrometry, subatmospheric pressure flames will be emphasized. This will permit spatial extension of soot formation stages which will ease resolution requirements for both optical and mass spectrometric approaches. This could be very significant since, for example, Bittner and Howard (Ref. 28) have

R86-956545-F

shown recently that even at 20 Torr polycyclic aromatic hydrocarbons peak and occur within a few mm in a premixed benzene/oxygen/argon flame. Summarizing, the preceding more extended measurement approach to additive behavior will greatly enhance the prospect of unraveling the associated kinetics.

Iron measurements will be included in the above program, but further measurements of iron additive effects in diffusion flames will be done under UTC sponsorship.

## REFERENCES

1. Howard, J. B. and W. J. Kausch, Jr.: Soot Control By Fuel Additives. Prog. Energy Combust. Sci. 6, 263-276 (1980).
2. Haynes, B. S., H. Jander and H. Gg. Wagner: The Effect of Metal Additives on the Formation of Soot in Premixed Flames. Seventeenth Symposium (Internat.) on Combustion, The Combustion Institute, Pittsburgh, PA, pp. 1365-1374 (1979).
3. Bonczyk, P. A.: Measurement of Particulate Size by In-Situ Laser-Optical Methods: A Critical Evaluation Applied to Fuel-Pyrolyzed Carbon. Combust. Flame 35, 191-206 (1979).
4. Bonczyk, P. A.: In-Situ Optical Measurement of Additive Effects on Particulates in a Sooting Diffusion Flame. Combust. Flame 51, 219-229 (1983).
5. Verdick, J. F. and P. A. Bonczyk: Laser-Induced Saturated Fluorescence Investigations of CH, CN and NO in Flames. Eighteenth Symposium (Internat.) on Combustion, The Combustion Institute, Pittsburgh, PA, pp. 1559-1566 (1981).
6. Wolfhard, H. G. and W. G. Parker: A New Technique for the Spectroscopic Examination of Flames at Normal Pressures. Proc. Phys. Soc. 62A, 722-730 (1949).
7. Wolfhard, H. G. and W. G. Parker: A Spectroscopic Investigation into the Structure of Diffusion Flames. Proc. Phys. Soc. 65A, 2-19 (1952).
8. Kent, J. H., H. Jander and H. Gg. Wagner: Soot Formation in a Laminar Diffusion Flame. Eighteenth Symposium (Internat.) on Combustion, The Combustion Institute, Pittsburgh, PA, pp. 1117-1126 (1981).
9. Kent, J. H. and H. Gg. Wagner: Soot Measurements in Laminar Ethylene Diffusion Flames. Combust. Flame 47, 53-65 (1982).
10. Horvath, J. J., J. D. Bradshaw, J. N. Bower, M. S. Epstein, and J. D. Winefordner: Comparison of Nebulizer-Burner Systems for Laser-Excited Atomic Fluorescence Flame Spectrometry. Anal. Chem. 53, 6-9 (1981).
11. Maessen, Frans J. M. J., P. Coevert, and J. Balke: Comparison of Pneumatic Nebulizers in Current Use for Inductively Coupled Plasma Atomic Emission Spectrometry. Anal. Chem. 56, 899-903 (1984).

12. Ashton, A. F. and A. N. Hayhurst: Kinetics of Collisional Ionization of Alkali Metal Atoms and Recombination of Electrons with Alkali Metal Ions in Flames. *Combust. Flame* 21, 69-75 (1973).
13. Alkemade, C. Th. J., Tj. Hollander, W. Snelleman and P. J. Th. Zeegers: Metal Vapours in Flames, Pergamon, New York (1982).
14. Bonczyk, P. A.: Laser Detection of Combustion Species, in Analytical Laser Spectroscopy (S. Martellucci and A. N. Chester, Eds.), Plenum, New York, pp. 107-130 (1985).
15. Murad, E.: Thermochemical Properties of the Gaseous Alkaline Earth Monohydroxides. *J. Chem. Phys.* 75, 4080-4085 (1981).
16. Jensen, D. E. and G. A. Jones: Alkaline Earth Flame Chemistry. *Proc. R. Soc. Lond. A* 364, 509-535 (1978).
17. Cotton, D. H., N. J. Friswell and D. R. Jenkins: The Suppression of Soot Emission from Flames by Metal Additives. *Combust. Flame* 17, 87-98 (1971).
18. Ndubizu, C. C., and B. T. Zinn: Effects of Metallic Additives upon Soot Formation in Polymer Diffusion Flames. *Combust. Flame* 46, 301-314 (1982).
19. Feugier, A.: Effect of Metal Additives on the Amount of Soot Emitted by Premixed Hydrocarbon Flames. *Adv. Chem. Ser.* 166 (Evaporation-Combust. Fuels), 178-189 (1978).
20. Retrievi, K. E., J. P. Longwell, and A. F. Sarofim: The Effects of Ferrocene Addition on Soot Particle Inception and Growth in Premixed Ethylene Flames (unpublished manuscript).
21. Frazee, J. D., and R. C. Anderson: Effect of Ferrocene on Carbon Formation from Acetylene. *Fuel* 38, 329-331 (1959).
22. Jung-Chun, Yin: Eliminating Smoking in Combustion of Petroleum Hydrocarbons by Ferrocene and Synthesis of Ferrocene. *Chemical Abstracts* 94, 124292g (1981).
23. Kracklauer, J. J.: Conditioning Diesel Engines. *Chemical Abstracts* 99, 73651s (1983).

24. Klarman, A. F.: Evaluation of Extended Use of Ferrocene for Test Cell Smoke Abatement; Engine and Environmental Test. Naval Air Propulsion Test Center Report No. NAPTC-PE-110, Trenton, New Jersey, October (1977).
25. Michel, A., M. Bert, Tran Van Hoang, P. Brussiere, and A. Guyot: Main Functions of Iron Compounds as Smoke Suppressant in Poly (vinyl Chloride) Combustion. *J. Appl. Polymer Sci.* 28, 1573-1584 (1983).
26. Abdel-Khalik, S. I., T. Tamaru, and M. M. El-Wakil: A Chromatographic and Interferometric Study of the Diffusion Flame around a Simulated Fuel Drop. Fifteenth Symposium (Internat.) on Combustion, The Combustion Institute, Pittsburgh, PA, pp. 389-399 (1974).
27. Bulewicz, E. M., D. G. Evans and P. J. Padley: Effect of Metallic Additives on Soot Formation Processes in Flames. Fifteenth Symposium (Internat.) on Combustion, The Combustion Institute, Pittsburgh, PA, pp. 1461-1470 (1974).
28. Bittner, J. D. and J. B. Howard: Composition Profiles and Reaction Mechanisms in a Near-Sooting Premixed Benzene/Oxygen/Argon Flame. Eighteenth Symposium (Internat.) on Combustion, The Combustion Institute, Pittsburgh, PA, pp. 1105-1116 (1981).



**UNITED  
TECHNOLOGIES  
RESEARCH  
CENTER**

East Hartford, Connecticut 06108

APPENDIX I

SUPPRESSION OF SOOT IN FLAMES BY ALKALINE-EARTH  
AND OTHER METAL ADDITIVES\*

P. A. Bonczyk  
United Technologies Research Center  
East Hartford, Connecticut 06108

Submitted for Publication  
in COMBUSTION SCIENCE and TECHNOLOGY  
July, 1986

\*Jointly sponsored by the Air Force Office of Scientific Research (AFOSR) and the Environics Division of the Air Force Engineering Services Center (Tyndall AFB, Fla.) under AFOSR Contract F49620-83-C-0113.



## ABSTRACT

Experiments were performed to clarify the role of metallic fuel additives in relation to soot suppression in a well defined laboratory-scale diffusion flame. Principal emphasis was given to three alkaline-earth metals; namely, Ba, Sr and Ca. The experiments included Cu, Sn, Li, Na and K measurements as well, but only to the extent that the latter contributed to understanding the details of alkaline-earth behavior. The additives were in the form of aqueous solutions of salts of the preceding metals. The solutions were aspirated into the oxidant flow of a nearly two-dimensional laminar  $C_2H_4$ /air flame emanating from a symmetric Wolfhard-Parker burner. Nonperturbing spatially precise laser/optical techniques were used to measure flame temperature, as well as to characterize soot, metal and radical species throughout the flame. The flame temperature was measured via sodium line reversal. Soot size, number density and volume fraction were determined from Mie scattering. Insofar as possible, the metal and radical species concentrations were inferred from optical absorption, optical emission or laser-induced fluorescence, as applicable; however, in order to determine all the metal species concentrations of interest, the measurements were supplemented by numerical estimates using known equilibrium constants for the metal/radical reactions occurring in the flame. The alkaline-earth metals were observed to alter the three soot parameters above in accordance with a  $Ba > Sr > Ca$  order of effectiveness and, moreover, the effectiveness was a strong function of measurement position. The temperature and species measurements were used to relate this variation to a specific metal combustion product. Following this approach, a conclusion is reached which strongly implicates the charged  $MOH^+$  ( $M = Ba, Sr, Ca$ ) species as responsible for soot suppression. In addition, since significant suppression

may occur with only a slight size change, the metal principally reduces the soot number density, which suggests inhibitory intervention at an early soot formation stage.

## 1. INTRODUCTION

The appearance of soot in combustion processes may have significant negative consequences. It is an atmospheric pollutant which is strongly suspected of being injurious to human health. Further, from an industrial engineering perspective, soot may cause premature degradation and, ultimately, the failure of a combustor due to increased and excessive heat transfer to its liner surfaces. In the near future, these problems may be aggravated even further with the use of heavily sooting, shale or coal derived, alternative fuels. One approach for eliminating soot is to develop a smokeless combustor. It is not clear, however, that this is a realizable objective in the near future since the mechanisms accompanying soot formation are still poorly understood and fuel quality is changing continuously. An economical, effective and convenient way to control soot formation is to use fuel additives. The current difficulty with additives is that their precise mode of action in suppressing soot is not clear. This, unfortunately, has made the evaluation and selection of specific additives more difficult, and consequently has slowed their application to potentially useful areas. In this paper, an experiment is described which attempts to clarify the details of fuel additive behavior in relation to soot suppression.

Research in the fuel additives area up to the year 1980 has been reviewed very adequately by Howard and Kausch (1980). The latter review summarizes additive use in both laboratory and practical combustion media. More recently, additive measurements have been made in stationary aircraft engines (Naval Environmental Protection Support Service, Aircraft Environmental Support Office, Naval Air Systems Command, 1983), a dilute swirl combustor (Samuelson et al., 1983), a single spray combustor (Okada, 1983), and in laboratory diffusion flames (Ndubizu and Zinn, 1982; Bonczyk, 1983, 1984 and 1985). For the most part, past experiments have been qualitative in nature.

They have served, for example, to establish the effectiveness of barium, iron, manganese and other metal compounds as soot suppressants in diverse combustion media. Due to emphasis on postcombustion sampling, etc., they have done little, however, to aid in understanding additive behavior in detail. There have been two recent exceptions to this general trend. In one case, Haynes et al. (1979) used in-situ laser/optical techniques to determine the effects of alkali and alkaline-earth metals on soot size, number density and volume fraction throughout premixed ethylene/air flames of varying stoichiometry. These data yielded semi-quantitative conclusions concerning additive mechanisms; namely, alkali metals were shown to suppress soot electrically, whereas for alkaline-earth metals the suppression was both electrical and (possibly) chemical in origin. In a second experiment emphasizing in-situ laser/optical techniques as well, Bonczyk (1983) showed that alkali metal additives alter soot size and number density, but may or may not reduce the soot loading depending on the mole fraction of alkali cations present. This experiment was done in a laminar  $C_3H_8/O_2/N_2$  diffusion flame; it confirmed the importance of electrical factors for alkali metals as suggested earlier by Haynes et al. (1979). Although both preceding experiments represent a significant advance beyond previous approaches, they are less than adequate with respect to firmly identifying the particular metal species responsible for soot suppression and the combustion stage(s) at which the metal intervenes. In this paper, an experiment is described which attempts to correct these inadequacies.

The experiments described below involve the measurement of alkaline-earth metal additive effects in a sooting, laminar  $C_2H_4$ /air diffusion flame. In contrast with previous experiments, an attempt was made to measure both soot and metal species using nonperturbing spatially precise optical methods. In

this way, it was possible to relate a specific metal species to soot suppression, as well as to determine the relatively complex behavior of the additive throughout the flame. A diffusion flame was selected for study since this choice complements the study of Haynes et al. (1979), extends the earlier work of Bonczyk (1983), and relates more readily to practical combustion media than a premixed flame does.

## 2. EXPERIMENT

The apparatus used to make the fuel additive measurements is shown schematically in Figure 1. With it, soot particulate parameters were characterized with and without flame seeding, and metal species concentrations, as well as flame temperature, were measured. A detailed description of both the apparatus and the experimental approach follow below.

### 2.1 FLAME AND ADDITIVE SEEDING

In Figure 1, B is a burner (Wolfhard and Parker, 1949; Kent and Wagner, 1982) having a central 5 x 45 mm fuel slot, two adjacent symmetrically positioned 10 x 45 mm oxidant slots, and a metal shroud enclosure. The gas flows to the burner are: 229 cc/min ethylene + 247 cc/min nitrogen to the fuel slot; 2.87 liters/min air to each oxidant slot; 50.4 liters/min air to the shroud (72 cm<sup>2</sup> cross-sectional area). These flows are such that the diffusion flame is highly overventilated and, hence, the two flame sheets are folded inward toward a common apex. This flame, whose end view is shown in Figure 2a, is roughly 40 mm in height and 5 mm wide at its base.

Additives are introduced by pneumatically aspirating an aqueous solution of a metallic salt into the oxidant flow stream using a Varian #99-100236-00 adjustable nebulizer (Willis, 1967; Browner and Boorn, 1984). It requires a (2-3) liter/min carrier gas flow rate for threshold operation, and near 5 liters/min for optimum performance. For this reason, the air flows to the nebulizer and to the oxidant slots are one and the same (= 5.74 liters/min). The nebulizer flow requirements preclude additive insertion into the fuel stream since then a flame completely altered from that in Figure 2a would result; however, insertion into either the air or fuel streams is equivalent since rapid diffusion transverse to the flow axis assures uniform additive

dispersal. This was verified by seeding the flame with NaCl, and then inferring a constant Na-atom concentration in a lateral direction, at 8 mm height and above, from the absorption of laser light at 5890 Å, which corresponds to the atom's  $3s(^2S_{1/2}) + 3p(^2P_{3/2})$  transition.

An end view of a very heavily seeded flame is shown in Figure 2b. As discussed below, the green/yellow emission is due principally to Ba, BaO and BaOH spectra.

## 2.2 SOOT MEASUREMENTS

Soot is measured with and without additives present using the 10 nsec, 10 pps Nd:Yag laser in Figure 1, as well as the two detection arms oriented at 20 and 160° with respect to the incident light direction. The Pellin-Broca prism, PBP, serves two purposes. It rotates the 5320 Å 2x Nd:Yag laser output by 90°, and refracts the 10,600 Å 1x Nd:Yag residual output into the light traps, T. The half-wave plate,  $\lambda/2$ , rotates the polarization axis of the laser to a direction normal to the scattering (or Figure 1) plane. Twenty percent of the 5320 Å radiation is passed by the splitter, BS, to the reflecting mirror, M1, and then to the glass plate, G. Then, the reflected light is focussed by lens L1 into the flame at B. The arms at 20 and 160° record the light Mie scattered by the soot particulates. Each detection arm has two apertures, A, to define both the optical sample length and the light collection solid angle, a polarization analyzer, P, aligned with the laser polarization axis, a narrow-band filter, F, centered at 5320 Å, and a photomultiplier, PMT. Electronic processing of all PMT signals is done with EG&G/Princeton Applied Research boxcar averagers not shown in Figure 1.

Soot size, number density and volume fraction are inferred from the light intensities at the PMT's #1 and #2. The soot diameter,  $D$ , is evaluated from the  $20/160^\circ$  intensity ratio (Bonczyk, 1979). Having  $D$ , the number density,  $N$ , is obtained from the absolute intensity at either angle. Then, the volume fraction,  $f_v$ , is calculated from,  $f_v = (\pi D^3/6)N$ . In the Mie analysis, particulate nonsphericity is neglected, a monodisperse size distribution is assumed, and the refractive index is taken to be,  $\hat{n} = 1.94 - 0.66i$  (Senftleben and Benedict, 1918). In earlier work (Bonczyk, 1979), it was shown that an unambiguous size distribution determination is not possible for small, high number density nonspherical particulates whose refractive index is not accurately known. This accounts for the monodisperse assumption above, which in fact has no significant bearing in relation to understanding additive behavior.

### 2.3 METAL SPECIES MEASUREMENTS

For metal species measurements, the techniques used were laser absorption or induced-fluorescence, as well as optical emission. For absorption and fluorescence, the wavelength tunable dye laser in Figure 1 is used, its output being directed to B via mirrors, M2, and lens, L1. In the case of absorption, the transmitted light is recollimated by the lens, L2, attenuated by the neutral density filter, NDF, and directed via a fiber optic cable to a second spectrometer/PMT combination (not shown). In the case of fluorescence, the light is collected at  $90^\circ$  with lenses, L3, and the dove prism, DP. The lenses image the flame in the plane of the spectrometer slit with 1x magnification, and the prism rotates the image by  $90^\circ$ . In this way, the thin laser/metal interaction line is collinear (not orthogonal) with the vertical spectrometer slit, thereby optimizing the signal intensity. For emission measurements,



a lens, L2, is selected such that the Figure 2b end view of the flame is imaged in the plane of a  $10^{-2}$  cm diam aperture with 1x magnification; the aperture replaces the NDF in Figure 1.

#### 2.4 TEMPERATURE MEASUREMENTS

Flame temperatures were measured by standard sodium-line reversal procedures (Gaydon and Wolfhard, 1979). The background light source required for this measurement was a tungsten filament lamp. Since both the radiant filament and the flame were imaged in the plane of the aperture mentioned above, temperatures were measured with approximately  $10^{-2}$  cm spatial resolution. Sodium was introduced into the flame using the nebulizer described above; however, in this case the level of seeding was very slight so as not to perturb the soot loading and, hence, the flame radiance. Representative temperature profiles are shown in Figure 3.

### 3. RESULTS

#### 3.1 SOOT

Initially, soot measurements were made at a single point in the flame for a variety of metal additives. This was done in order to compare the soot suppressing properties of the alkaline-earths with other metals. The coordinates of the point chosen were (mm),  $(x,z) = (1,23)$ . This point is laterally located just inside the flame's luminous periphery, and vertically at roughly two-thirds of its overall height. The  $x = 1$  mm lateral coordinate coincides with a peak in the soot volume fraction, which yields strong Mie signals with and without additives present. The results for the various metals are given in Table I. In each case, the metal was introduced by aspirating a 0.2 molar MCl or  $MCl_2 \cdot nH_2O$  ( $M$  = metal atom;  $n = 1,2$  etc.) solution. The choice of a chloride salt is significant only to the extent that its water solubility is high. This is the case since the metal constituent alone is responsible for altering soot, which was verified by observing that  $Ba(CHO_2)_2$ ,  $Ba(OOCCH_3)_2$ ,  $Ba(NO_2)_2 \cdot H_2O$  and  $BaCl_2 \cdot 2H_2O$  all suppress soot very nearly equally. Table I gives soot size, number density and volume fraction with an additive present ( $= D, N$  and  $f_v$ ), normalized to the corresponding values at zero molarity with water alone present ( $= D^0, N^0$  and  $f_v^0$ ). The measurement precision of the ratios in Table I is roughly  $\pm 10\%$ . With this in mind, the metals Sr, Ba, Na and K are seen to be soot suppressants, while the other metals are not. In data not included here, as expected the degree of soot suppression by the former metals increased or decreased in direct relation to the solution's molar strength. The wide disparity in metal additive behavior in Table I has been observed qualitatively in earlier work (Cotton, Friswell and Jenkins, 1971). The three alkaline-earth metals, which are the principal subject of this work, had not

been studied previously in diffusion flames. Inclusion of the alkali metals provides a link with past work in an axisymmetric  $C_3H_8/O_2/N_2$  flame (Bonczyk, 1983). Finally, the particular significance of Cu and Sn in Table I will be made more apparent below.

In order to examine additive behavior more fully, the alkaline-earth measurements above were extended to include other locations in the flame. Generally, the results of these measurements were as follows. At roughly two-thirds or less of the overall flame height, the additive effectiveness varied very significantly in a lateral direction. It was a minimum at the burner center, but increased sharply away from the center in the direction of the flame periphery. Additive behavior varied with vertical measurement position as well. For  $x = 0$  (burner center) and variable height, the metals reduced soot only at and within 5 to 10 mm of the flame apex. These spatial mappings of additive behavior are shown in more detail in Figures 4, 5 and 6.

The effect of a Sr salt additive on soot  $D^\circ$ ,  $N^\circ$  and  $f_v^\circ$ , for fixed vertical and variable lateral positions, is shown in Figures 4a, 4b and 4c, respectively. As mentioned above, additive effectiveness has a strong lateral dependence for all three soot parameters. Also, the effectiveness increases in the direction of increasing flame temperature, the partial profile of which is shown in Figure 4 as well. Finally, since in Figure 4a the additive's effect on diameter is small, the substantial reduction in volume fraction in Figure 4c is due primarily to the large decrease in number density evident in Figure 4b. Equivalently, this means that for a 0.2 molar or weaker solution, or (roughly) a  $10^{12} \text{ cm}^{-3}$  or smaller total metal species concentration in the flame, the principal action of the Sr metal is to decrease the number of soot particulates present. This contrasts with the behavior of alkali metal

additives, potassium in particular, which has been shown (Table I and Bonczyk, 1983) to reduce  $D^*$  strongly and to increase (or decrease)  $N^*$  in hydrocarbon/air diffusion flames.

In order to examine the lateral dependence of additive behavior further, metals other than Sr were studied as well. These results are summarized in Figure 5, which gives the lateral dependences of the effect of Ca, Sr, Ba and Na on soot volume fraction. The data in each case are for a 0.1 molar salt concentration; as such, it should be noted that differences between the data in Figure 4c and the Sr data in Figure 5 are due to dissimilar  $SrCl_2 \cdot 6H_2O$  concentrations. It is evident from Figure 5 that the three alkaline-earth metals behave similarly, with the important exception that, as concerns soot suppressing effectiveness,  $Ba > Sr > Ca$  at all lateral positions. Sodium suppresses soot at the burner center and, in general, its lateral behavior is significantly different from those of the alkaline-earths. This, however, is not entirely surprising since, as will be made apparent below, the thermochemistries of alkali and alkaline-earth metals are not the same in flames. As concerns understanding alkaline-earth behavior, the significant features of the data in Figure 5 are: 1) the pronounced lateral dependence of soot suppression; 2) the  $Ba > Sr > Ca$  order of effectiveness.

The Ba data in Figure 5 show no soot suppression at the  $x = 0$  burner center position. This is not the case, however, for all vertical positions. In Figure 6, for example, the normalized volume fraction is given as a function of height in the flame for the same Ba additive as in Figure 5. In agreement with the data in Figure 5, there is no effect on soot at  $(x, z) = (0, 23 \text{ mm})$ , but for  $z > 23 \text{ mm}$  there is a reduction in soot which appears most pronounced near the flame tip. The apparent increase of volume fraction in the  $20 < z < 28 \text{ mm}$  region in Figure 6 is less than the measurement

error and, therefore, is without particular meaning. Taken together, Figures 5 and 6 indicate, then, that the alkaline-earth metals are most effective in the vicinity of the main reaction zone of the flame.

### 3.2 METAL SPECIES

In order to understand the behavior of alkaline-earth metals in relation to soot suppression, it is at least necessary to identify the several different metal species present in the flame and to estimate their relative concentrations. There is evidence from past work that a flame seeded with alkaline-earth metal salts contains the following metal combustion species: M, MO, MOH,  $M(OH)_2$ ,  $M^+$  and  $MOH^+$  (M = Ba, Sr, Ca, etc.). This has been discussed by Jensen and Jones (1978), wherein literature citations of past, relevant work may be found. For the work described here, M, MO, MOH and  $M(OH)_2$  were verified as present in the flame from their observed, known (Mavrodineanu and Boiteux, 1965) emission spectra. The  $M^+$  have known spectra as well and were assumed to be present, but could not be observed due to weak optical emission resulting from low species concentration and the relatively cool  $\sim 2000$  K flame temperature. The  $MOH^+$  spectra, if they exist, are unknown; consequently, the latter species also were not observed directly. An example of this species identification is given in Figure 7, where a portion of the observed emission spectra for a Ba seeded flame is shown. The numerals in parentheses identify various BaO upper and lower vibrational states to which the low resolution band spectra correspond. Also evident is the Ba atomic emission at 5535 Å; the Na atomic line is due to an impurity present at a concentration which is insignificant with respect to Na suppression of soot.

In flames (and other media), the absolute concentrations of atomic, molecular and radical species may be determined, in principle, by the method of saturated laser-induced fluorescence (Bonczyk and Shirley, 1979; Verdick

and Bonczyk, 1981; Bonczyk, 1985). Discussion of this technique is omitted here, except to emphasize that significant saturation of the fluorescence intensity is critical to its implementation. Saturation occurs at high laser excitation intensities, and becomes apparent when the relation between laser and fluorescence intensities makes a transition from linear to nonlinear behavior. The particular value of saturation is that quenching corrections to the measured fluorescence intensity, which are often very difficult to estimate, need not be made, thereby greatly simplifying the evaluation of species concentrations. Initially, the approach taken in this work was to attempt to use saturated fluorescence to estimate the concentrations of the M, MO, etc. species mentioned above. An example of such a measurement is given

Figure 8, where fluorescence intensity as a function of lateral position is given for SrOH. As mentioned, the fluorescence intensity may be converted to a concentration only if significant saturation is present; this, however, was not observed to be the case for all lateral positions in Figure 8. This is apparent in Figure 9 where fluorescence intensity versus laser energy is given for two different lateral positions. At  $x = 3.5$  mm, which is outside the luminous soot zone, there is sufficient saturation; but at  $x = 0$  mm, which is inside the soot zone, the saturation is significantly less and not sufficient for reliable concentration estimation. This difficulty with weak saturation, and further problems with use of the technique in connection with alkaline-earth species measurement in particular, are discussed below in somewhat more detail. In order to cope with the problem outlined immediately above, a different approach was adopted.

As an alternative to saturated fluorescence measurement of M, MO, MOH,  $M(OH)_2$ ,  $M^+$  and  $MOH^+$  for Ca, Sr and Ba (a total of 18 species!), the following equally valid approach was taken for the neutral species. In flames, these

species are involved in the balanced reactions (Schofield and Sugden, 1965; Cotton and Jenkins, 1968).



Since ions represent an insignificant fraction of the total metal concentration,  $[M]_0$ , the number balance among species is approximately given by

$$[M]_0 = [M] + [MO] + [MOH] + [M(OH)_2]. \quad (5)$$

Using Eqs. (1) through (5), it may be shown that the concentrations of individual species may be expressed in terms of  $[M]_0$  as follows (Hayhurst and Kittelson, 1974).

$$[M] = A[M]_0 \gamma^2 / (1 + B\gamma + AD\gamma^2), \quad (6)$$

$$[MO] = AC[M]_0 \gamma^2 / (1 + B\gamma + AD\gamma^2), \quad (7)$$

$$[MOH] = B[M]_0 \gamma / (1 + B\gamma + AD\gamma^2), \quad (8)$$

$$[M(OH)_2] = [M]_0 / (1 + B\gamma + AD\gamma^2), \quad (9)$$

where the constants A, B, C and D are given by

$$A = (1/K_1 K_2) ([H]_{eq} / [H_2O])^2; \quad C = K_3 [H_2O] / [H_2],$$

$$B = (1/K_2) ([H]_{eq} / [H_2O]); \quad D = 1 + C.$$

$\gamma$  is the ratio  $[H]/[H]_{eq}$  of the actual atomic hydrogen concentration to its equilibrium value, or, since reaction (4) is balanced,  $[OH]/[OH]_{eq}$ . The K's are equilibrium constants for reactions (1) through (3), and reliable values

for these constants, including their temperature dependence, are available in the published literature (Jensen and Jones, 1978). It follows, then, that fractional concentrations such as  $[M]/[M]_0$  may be determined provided that  $[H]/[H_2O]$  is measured and the temperature is known.

Hydrogen atom concentrations were determined in the ethylene/air flame using the sodium/lithium comparison method. This technique involves the measurement of Na and Li optical emissions, along with the use of two appropriate equilibrium relations very similar to Eq. (1) above. Further discussion of this well known method of H measurement is omitted here; additional details are available elsewhere (Alkemade et al., 1982). Figure 10 gives the lateral dependence of  $[H]/[H_2O]$  at 18 mm height, which is precisely the parameter required to calculate the fractional species concentrations mentioned above. Similar data were obtained at 23 mm height as well. Since  $[H_2O]$  is expected to be significantly less sensitive to temperature variation than the H (or OH) radical (Smyth et al., 1985), the data in Figure 10 nearly give the lateral variation of  $[H]$  within a proportionality constant. Several assumptions are inherent in the approach described above, including local equilibrium in the diffusion flame. Despite this, however, the  $[H]/[H_2O]$  numerical values and the near spatial coincidence of radical and temperature peaks are about as expected.

Results for neutral species concentrations at 23 mm height are given in Table II. The numerals in parentheses are powers of ten; hence,  $[M]/[M]_0 = 4.4 \times 10^{-2}$  for Ca, etc. The total metal concentration,  $[M]_0 \sim 10^{12} \text{ cm}^{-3}$ , has been estimated from  $[Na] \sim [Na]_0$  optical emission measurements of sodium atom concentration in a flame seeded with a NaCl



solution at the same 0.2 molar strength as the alkaline-earths. In order to check the validity of the results shown in Table II, independent determinations of  $[M]$  were made from optical emission measurements. Although agreement between absolute concentrations was very good for Sr and only fair for Ba and Ca, the order  $[Sr] > [Ca] > [Ba]$  in Table II was verified by the latter independent procedure. Results for the significant charged species concentrations are given in Table II as well. The concentration values were determined by: 1) assuming the chemi-ionizing reaction,  $M + OH \rightarrow MOH^+ + e^-$ , to be balanced in the flame; 2) taking equilibrium constants for the reaction from earlier work (Jensen and Jones, 1978); 3) using values of  $[M]$  and  $[OH]$  (Bonczyk, 1986) determined from emission and saturated laser-induced fluorescence measurements, respectively.

#### 4. ANALYSIS

The significant question to ask with regard to Table II is whether one or more of the five species types have relative Ca/Sr/Ba concentrations suggestive of the  $Ba > Sr > Ca$  order of soot removal discussed above and evident in Figure 5. From Table II, this is the case for  $[MO]$  and  $[MOH^+]$ , which appears to implicate one or both species as soot suppressants; however, as will be apparent in the discussion which follows,  $[MOH^+]$  is the more likely candidate.

The thermochemistries of several elementary carbon oxidation reactions involving neutral metal species are shown in Table III. The choice of reactions should not be construed as definitive, especially since solid carbon oxidation is not likely to be an elementary process kinetically. Instead, the intent here is to consider the few simple, representative reactions in Table III which have appeared previously in the open literature: Eq. (1) (Fruehan and Martonik, 1976; Hellmold and Gordziel, 1983); Eq. (2) (McKee, 1982); Eq. (3) (Hellmold and Gordziel, 1983; Grayson and Eckroth, 1978). Using thermodynamic tables (Stull and Prophet, 1971), the energies of enthalpy ( $\Delta H$ ) and the Gibbs (or free) energies ( $\Delta G$ ) have been calculated for these reactions at 298 and 2000 K, respectively. Discussion here will be limited to the more meaningful Gibbs energies, and to Eqs. (1) and (2) since sufficient thermodynamic data are not available to calculate the Gibbs energies for (3). The results in Table III are not suggestive of  $Ba > Sr > Ca$  soot removal. Reaction (1) proceeds spontaneously for the alkaline-earths, but the relative degree of spontaneity is inverse to the soot removal order, and reaction (2) is even less suggestive of the latter order. Further evidence that reactions (1) and (2) are not responsible for soot removal follows from experiments done in our flame with lithium (Li) and tin (Sn) chloride additives. In a variety

of flames, it has been shown that the major species in the case of Li and Sn seeding are LiOH and SnO, respectively (Halls, 1977; Bulewicz and Padley, 1971). Yet despite the preponderance of the latter species, and the favorable Gibbs energies for Sn relative to Ba in reaction (1), and Li relative to Ba in reaction (2), neither lithium nor tin perturbed soot in our flame.

The preceding discussion is intended as evidence suggesting that neutral metal species are not responsible for soot removal. In contrast, the following convincing argument may be given for the importance of ions, specifically  $\text{MOH}^+$ . There are a variety of routes by which  $\text{MOH}^+$  may be formed (Hayhurst and Kittelson, 1974). One of the two most favorable ionization paths, already mentioned above, is shown in Table IV. For it, the rate of ion production is seen to be proportional to the cube of the H concentration and to follow the order  $\text{Ba} > \text{Sr} > \text{Ca}$ . This is significant for two reasons. First, from Figure 10 it follows that  $d[\text{MOH}^+]/dt$  has a very pronounced lateral dependence, in agreement with that for additive effectiveness in Figures 4 and 5. Second, the relative magnitudes of  $d[\text{MOH}^+]/dt$  for Ca, Sr and Ba agree with their relative soot removal efficiencies. Final evidence for the importance of the  $[\text{MOH}^+]$  is given in Table V. Therein, soot reduction,  $f_v/f_v^\circ$ , is tabulated for the various metals tested as additives in the present work. From top to bottom in Table V, the metals are arranged in descending order of their respective ionization potentials. Since the number of ions present increases with decreasing ionization potential, the metals are arranged from top to bottom in ascending order of cation concentration. Accordingly, Table V shows clearly that soot reduction is strongly correlated with the number of cations present, and specifically for alkaline-earths the number of  $[\text{MOH}^+]$  present.

## 5. CONCLUDING REMARKS

### 5.1 ADDITIVE MECHANISMS

In this work, evidence has been presented which strongly suggests that  $[\text{MOH}^+]$  are the critical species as concerns the suppression of soot by alkaline-earth metal fuel additives. This is a significant conclusion, but it represents only the first step toward understanding the additive mechanism in detail. For example, such an understanding requires information concerning the one or more soot formation stages at which the metal intervenes. For the laser/optical Mie scattering approach used in this work, it is possible to reach definitive conclusions concerning late stages, but only inferences are possible regarding early stage intervention. The reason for this limitation is that Mie scattering is only applicable to particulates which are a few tens-of-Angstroms or larger in size, and not for example to gaseous hydrocarbon species and smaller particulates present at early soot formation stages. Accordingly, the additive induced reduction in size for relatively large particulates ( $D^0 \sim 1500 \text{ \AA}$ ) observed in this work convincingly demonstrates intervention with particulate agglomeration. On the other hand, the strong additive perturbation of number density,  $N^0$ , suggests an effect on soot precursor species, but as mentioned, the present approach does not permit a definitive test of this conclusion. In order to cope with this difficulty, future work at this laboratory will make use of both optical and mass spectrometric techniques to measure the effects of additives on soot. For species determination, optical methods will remain the first choice due to their in-situ and spatially precise nature, but as pointed out above there are instances where laser/optical approaches are not applicable. In such cases, recourse will be made to mass spectrometry as a necessary and highly useful alternative. For example, laser/optical techniques will be used to characterize particulate parameters down to approximately  $(10-30) \text{ \AA}$  in size,

to measure concentrations of additive species with known spectra, and finally where applicable to measure concentrations of significant unseeded flame species like, e.g., the hydroxyl radical. Mass spectrometry, on the other hand, will be used to probe important species without known optical spectra, such as soot precursors and intermediates as well as additive species.

In Figure 5, soot volume fraction reduction by alkaline-earth metals has a much more pronounced lateral dependence than is the case for Na. This latter difference is, however, not entirely surprising since the thermochemistries of alkali and alkaline-earth metals are significantly different. For the alkalis, species formation is governed approximately by  $M + X \rightleftharpoons M^+ + e^- + X$ , where X is a dominant foreign collision partner and  $M = \text{Li, Na, K, etc.}$  (Hayhurst and Kittelson, 1974). In this case, the lateral variation of  $[M^+]$  (or the equilibrium constant of the preceding reaction) is determined principally by the associated temperature variation across the flame. In contrast, from Eqs. (1), (2) and (3) above, and Table IV, the alkaline-earth concentrations depend on both temperature and  $[H]$  (or  $[OH]$ ), which results in a stronger lateral variation of  $[MOH^+]$ .

There have been repeated speculations in the published literature concerning a possible chemical/OH explanation of alkaline-earth metal behavior in relation to soot suppression (Cotton et al., 1971; Ndubizu and Zinn, 1982; Feugier, 1978). The soot reduction is presumed to occur via a metal-induced catalytic increase in OH, which in turn increases the rate of soot oxidative burn out given by  $C_{\text{solid}} + OH \rightarrow CO + (1/2)H_2$ . The first quantitative test of this mechanism was carried out recently at this laboratory (Bonczyk, 1986). The results of this work do not support the above mechanism as a viable explanation of alkaline-earth behavior. The OH concentrations were inferred

from saturated laser-induced fluorescence measurements. The exciting light near 3090 Å was obtained by frequency doubling the output of a visible, pulsed dye laser. The effect of the additive was to reduce the OH concentration to a degree dependent upon the particular metal selected, i.e. Ca, Sr or Ba, and the lateral measurement position. Significantly, therefore, there was no evidence of additive enhancement of OH concentration and consequent more rapid soot oxidative burn out as previously has been suggested; this conclusion was valid for various vertical and lateral positions in the flame.

## 5.2 OPTICAL TECHNIQUE LIMITATIONS

The purpose of this discussion is to summarize the strengths and limitations of the laser/optical approach as applied to the research described here. It will be apparent that certain limitations do indeed exist, and that in some cases they may be circumvented only by recourse to alternative methods.

Mie scattering is a very powerful method of in-situ characterization of soot particles in flames (Bonczyk, 1979), but for very small particles of insufficient quantity the Mie intensities can be obscured by Rayleigh scattering of laser light by the ambient gas. This occurs since the laser, Mie and Rayleigh wavelengths are all the same and, hence, discrimination between the latter two is very difficult. It may be shown that the ratio of Mie to Rayleigh intensities is given by  $I_{\text{Mie}}/I_{\text{Ray}} = (\lambda/2\pi)^2 i N/n(\partial\sigma/\partial\lambda)$ , where:  $I_{\text{Mie}}$  and  $I_{\text{Ray}}$  are the Mie and Rayleigh scattered intensities, respectively;  $\lambda$ , the wavelength of the incident laser radiation; "i", for  $\pi D/\lambda \geq 1$  ( $D$  = particle diameter), a complicated function of scattering angle, particle size and refractive index;  $N$ , the soot particle number density;  $n$ , the number density of Rayleigh scatterers;  $(\partial\sigma/\partial\lambda)$ , the Rayleigh differential scattering cross-section. It may be shown as well that for  $\pi D \ll 1$ , "i" varies as  $D^6$

(Kerker, 1969). Accordingly, as the particle size decreases, the above ratio sharply decreases as well since the denominator remains constant. In practice, this has meant, for example, that D'Alessio et al. (1974) were able to detect soot particles down to only  $D = 50 \text{ \AA}$  in an atmospheric pressure premixed  $\text{CH}_4/\text{O}_2$  flame.

The above example is an interference effect which limits the accuracy and range of particle measurement, but there are sources of interference with atomic and molecular measurements as well. A pointed example is the competition between Mie scattering from soot particles and laser-induced fluorescence (LIF) signal intensities during measurement of alkali and alkaline-earth atomic species concentrations. For alkali atom LIF, excitation and fluorescence measurement may be made to occur at two different wavelengths; hence, interference from Mie scattering at the excitation wavelength may be circumvented. For atomic sodium for example, the fluorescence  $3p(^2P_{1/2}) \rightarrow 3s(^2S_{1/2})$  at  $5895.9 \text{ \AA}$  may be observed following the excitation  $3s(^2S_{1/2}) \rightarrow 3p(^2P_{3/2})$  at  $5890.0 \text{ \AA}$ . In flames at 1 atm or higher pressure, the transfer  $3p(^2P_{3/2}) \rightarrow 3p(^2P_{1/2})$  results from collisions with ambient flame species, and the preceding  $\sim 6 \text{ \AA}$  excitation/fluorescence separation is sufficient to discriminate against Mie scattering. A similar positive conclusion may be shown to exist for other alkali atoms. Unfortunately, the preceding argument does not hold for alkaline-earth atoms. In the case of atomic barium for example, both excitation and fluorescence occur at one and the same wavelength, as in  $6s^2(^1S_0) \rightarrow 6s6p(^1S_0) \rightarrow 6s^2(^1S_0)$ , both at  $5535.5 \text{ \AA}$ . Finally, in some cases ambient gaseous species may interfere with LIF measurements as well. Omitting details and citing but one example, the flame species  $\text{C}_2$  has a  $\text{A}^3\Pi \rightarrow \text{X}^3\Pi$  Swan system with spectra in the interval  $(4365-6677) \text{ \AA}$  which overlaps the  $(4680-7097) \text{ \AA}$   $\text{BaO}$  spectra for the system  $\text{A}^1\Sigma \rightarrow \text{X}^1\Sigma$  (Pearse and Gaydon, 1976; Suchard, 1975).

There is an additional source of LIF interference which occurs if 1) soot is present and 2) the laser excitation intensity is high. This source of interference is laser modulated particulate incandescence which occurs when already incandescent soot particles absorb the incident laser light, heat to temperatures far above the ambient flame temperature and then emit greatly increased amounts of blackbody radiation. Since this occurs over a wide spectral range and in synchronism with the laser pulse, it is a noise source which is very difficult to discriminate against. It may be shown, for example, that this induced incandescence can raise the LIF detection limit for CH from 0.26 ppm in a clean flame to 80 ppm in a sooting flame, and similarly for OH from 0.32 ppm to 35 ppm (Eckbreth et al., 1978).

Another potential difficulty with optical methods is that frequently spectra of species of interest are poorly known, or in some cases may not exist at all. Further, even when spectra are known it is necessary for the application of LIF or optical absorption that: 1) wavelengths fall within the range of conventional and laser light sources; 2) individual lines in the spectra are resolved; 3) parameters such as molecular rotational constants and atomic/molecular transition oscillator strengths are known. Individual discussion of these factors is omitted.

In Table VI, the applicability of LIF to alkaline-earth species measurement is summarized; Table VI has been composed with reference, in part, to the preceding discussion. It should be emphasized that Table VI gives a worst case scenario in terms of species detection since optical absorption is not complicated by 4), and in some cases optical emission may be used to circumvent 3) for M detection. Moreover, the difficulties presented are representative and pertinent to alkaline-earth species, and do not necessarily carry over one-on-one to other species.



# ACKNOWLEDGEMENT

This research was jointly sponsored by the Air Force Office of Scientific Research (AFOSR) and the Environics Division of the Air Force Engineering Services Center (Tyndall AFB, Fla.) under AFOSR Contract F49620-83-C-0113.

## REFERENCES

- Alkemade, C. Th. J., Hollander, Tj., Snelleman, W., and Zeegers, P.J.Th. (1982). Metal Vapours in Flames, Pergamon, New York.
- Bonczyk, P. A. (1979). Measurement of Particulate Size by In-Situ Laser-Optical Methods: A Critical Evaluation Applied to Fuel-Pyrolyzed Carbon. *Combust. Flame* 35, 191.
- Bonczyk, P. A., and Shirley, J. A. (1979). Measurement of CH and CN Concentration in Flames by Laser-Induced Saturated Fluorescence, *Combust. Flame* 34, 253.
- Bonczyk, P. A. (1983). In-Situ Optical Measurement of Additive Effects on Particulates in a Sooting Diffusion Flame. *Combust. Flame* 51, 219.
- Bonczyk, P. A. (1984). Measurement of Fuel Additive Effects on Soot in Diffusion Flames. Poster Presentation at the Twentieth Symposium (Internat.) on Combustion, Ann Arbor, Michigan, 12-17 August.
- Bonczyk, P. A. (1985). Effects of Alkaline-Earth and Similar Metal Additives on Soot in Flames. Presented at the Combustion Institute Eastern Section Meeting, Philadelphia, PA, 4-6 November.
- Bonczyk, P. A. (1985). Laser Detection of Combustion Species. In Martellucci, S., and Chester, A. N. (Eds.), Analytical Laser Spectroscopy, Plenum, New York, pp. 107-130.
- Bonczyk, P. A. (1986). The Influence of Alkaline-Earth Additives on Soot and Hydroxyl Radicals in Diffusion Flames (to be published).
- Browner, R. F., and Boorn, A. W. (1984). Sample Introduction-The Achilles' Heel of Atomic Spectroscopy. *Analytical Chemistry* 56, 786A.
- Bulewicz, E. M., and Padley, P. J. (1971). Photometric Observations on the Behavior of Tin in Premixed  $H_2 + O_2 + N_2$  Flames. *Trans. Faraday Soc.* 67, 2337.
- Cotton, D. H., and Jenkins, D. R. (1968). Dissociation Energies of Gaseous Alkaline Earth Hydroxides. *Trans. Faraday Soc.* 64, 2988.
- Cotton, D. H., Friswell, N. J., and Jenkins, D. R. (1971). The Suppression of Soot Emission from Flames by Metal Additives. *Combust. Flame* 17, 87.

D'Alessio, A., di Lorenzo, A., Sarofim, A. F., Berretta, F., Masi, S., and Venitozzi, C. (1974). Soot Formation in Methane-Oxygen Flames. Fifteenth Symposium (Internat.) on Combustion, The Combustion Institute, Pittsburgh, PA, pp. 1427-1438.

Eckbreth, A. C., Bonczyk, P. A., and Verdick, J. F. (1978). Laser Raman and Fluorescence Techniques for Practical Combustion Diagnostics. Applied Spectroscopy Reviews 13, 15.

Feugier, A. (1978). Effect of Metal Additives on the Amount of Soot Emitted by Premixed Hydrocarbon Flames. Adv. Chem. Ser. 166 (Evaporation Combust. Fuels), 178.

Fruehan, R. J., and Martonik, L. J. (1976). The Rate of Reduction of MgO by Carbon. Metallurgical Transactions 7B, 537.

Gaydon, A. G., and Wolfhard, H. G. (1979). Flames: Their Structure, Radiation and Temperature, 4th Ed., Halsted Press (Wiley), New York, pp. 269-271.

Grayson, M., and Eckroth, D. (Eds.) (1978). Kirk-Othmer Encyclopedia of Chemical Technology, 3rd Ed., Wiley, New York, Vol. 4, p. 508.

Halls, D. J. (1977). The Efficiency of Atomisation of Sodium, Potassium and Lithium in the Air-Acetylene Flame. Spectrochimica Acta 32B, 397.

Hayhurst, A. N., and Kittelson, D. B. (1974). Ionization of Alkaline Earth Additives In Hydrogen Flames. II. Kinetics of Production and Recombination of Ions. Proc. R. Soc. Lond. A. 338, 175.

Haynes, B. S., Jander, H., and Wagner, H. G. (1979). The Effect of Metal Additives on the Formation of Soot in Premixed Flames. Seventeenth Symposium (Internat.) on Combustion, The Combustion Institute, Pittsburgh, PA, pp. 1365-1374.

Hellmold, P., and Gordziel, W. (1983). Untersuchungen zu den Teilreaktionen der Calciumcarbidbildung. Teil II. Untersuchungen zur Calciumcarbidbildung aus Calciumoxid und Kohlenstoff. Chemische Technik (Leipzig) 35, 297.

Howard, J. B., and Kausch, W. J., Jr. (1980). Soot Control By Fuel Additives. Prog. Energy Combust. Sci. 6, 263.

Jensen, D. E., and Jones, G. A. (1978). Alkaline Earth Flame Chemistry. Proc. R. Soc. Lond. A. 364, 509.

Kent, J. H., and Wagner, H. Gg. (1982). Soot Measurements in Laminar Ethylene Diffusion Flames. Combust. Flame 47, 53.

Kerker, M. (1969). The Scattering of Light and Other Electromagnetic Radiation, Academic Press, New York.

Mavrodineanu, R., and H. Boiteux, H. (1965). Flame Spectroscopy, Wiley, New York. (1965).

McKee, D. W. (1982): Gasification of Graphite in Carbon Dioxide and Water Vapor-The Catalytic Effects of Alkali Metal Salts. Carbon 20, 59.

Naval Environmental Protection Support Service, Aircraft Environmental Support Office, Naval Air Systems Command, Naval Air Rework Facility, North Island, California (1983). Cerium and Ferrocene Fuel Additive Tests on the TF41 and T56 Engines for Visible Emission Reduction. AESO Report No. 110-05-83, June.

Ndubizu, C. C., and Zinn, B. T. (1982). Effects of Metallic Additives upon Soot Formation in Polymer Diffusion Flames. Combust. Flame 46, 301.

Okada, H. (1983). Effects of Barium Compounds on Soot Formation in Single Spray Combustion. Oxidation Communications 4, 273.

Pearse, R. W. B., and Gaydon, A. G. (1976). The Identification of Molecular Spectra, 4th Ed., Halsted, New York.

Samuelson, G. S., Wood, C. P., and Jackson, T. A. (1983). Optical Measurements of Soot Size and Number Density in a Complex Flow, Swirl-Stabilized Combustor. Presented at the 62nd Symposium on Combustion Problems in Turbine Engines, Cesme, Turkey, October.

Schofield, K., and Sugden, T. M. (1965). Some Observations on the Ionization of Alkali and Alkaline-Earth Elements in Hydrogen Flames. Tenth Symposium (Internat.) on Combustion, The Combustion Institute, Pittsburgh, PA, pp. 589-604.

Senftleben, H., and Benedict, E. (1918). Über die Optischen Konstanten und die Strahlungsgesetze der Kohle. Annalen der Physik 54, 65.

Smyth, K. C., Miller, J. H., Dorfman, R. C., Mallard, W. G., and Santoro, R. J. (1985). Soot Inception in a Methane/Air Diffusion Flame as Characterized by Detailed Species Profiles. Combust. Flame 62, 157.

Stull, D. R., and Prophet, H. (Project Directors) (1971). JANAF Thermochemical Tables, 2nd Ed., U.S. Government Printing Office, Washington, June.

Suchard, S. N. (Ed.) (1975). Spectroscopic Data, Vol. 1, Part A, IFI/Plenum, New York.

Verdieck, J. F., and Bonczyk, P. A. (1981). Laser-Induced Saturated Fluorescence Investigations of CH, CN and NO in Flames. Eighteenth Symposium (Internat.) on Combustion, The Combustion Institute, Pittsburgh, PA, pp. 1559-1566.

Willis, J. B. (1967). Atomization Problems in Atomic Absorption Spectroscopy - I. A Study of the Operation of a Typical Nebulizer, Spray Chamber and Burner System. Spectrochimica Acta 23A, 811.

Wolfhard, H.G., and Parker, W. G. (1949). A New Technique for the Spectroscopic Examination of Flames at Normal Pressures. Proc. Phys. Soc. 62A, 722.

TABLE I. EFFECT OF DISSIMILAR METAL ADDITIVES ON SOOT

- i) Measurement position (mm):  $(x,z) = (1,23)$   
 ii)  $MCl$  or  $MCl_2 \cdot nH_2O$  ( $M$  = metal atom;  $n = 1,2$  etc.) solution molarity:  
 0.2  
 iii)  $(D, N, f_v)$  and  $(D^\circ, N^\circ, f_v^\circ)$ : soot diameter, number density and volume  
 fraction with and without additives respectively.

	$D/D^\circ$	$N/N^\circ$	$f_v^\circ/f_v$
Ca	1.04	0.90	1.00
Sr	0.91	0.39	0.27
Ba	0.79	0.19	0.10
Li	0.99	1.01	0.96
Na	0.72	1.39	0.52
K	0.50	0.96	0.12
Cu	1.00	1.03	1.03
Sn	1.01	0.96	1.00

TABLE II. ALKALINE-EARTH SPECIES CONCENTRATIONS

i) Measurement position (mm):  $(x, z) = (3, 23)$   
 ii)  $[M]_0: \sim 10^{12} \text{cm}^{-3}$

	<u>Ca</u>	<u>Sr</u>	<u>Ba</u>
$[M]/[M]_0$	4.4(-2)	6.9(-2)	9.0(-4)
$[MO]/[M]_0$	2.6(-3)	1.9(-2)	4.0(-1)
$[MOH]/[M]_0$	3.7(-1)	5.0(-1)	3.8(-1)
$[M(OH)_2]/[M]_0$	6.3(-1)	4.2(-1)	2.1(-1)
$[MOH^+]/[M]_0$	1.0(-2)	5.0(-2)	6.0(-2)

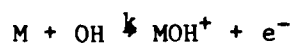
TABLE III. SOOT REDUCTION REACTION ENERGIES

	$\Delta H_{298}$ (kcal/mol)			$\Delta G_{2000}$ (kcal/mol)	
	(1)	(2)	(3)	(1)	(2)
Li		104.61			-7.66
Ca	5.93	94.16	-47.52	-54.59	-6.59
Sr	15.98	92.43	-43.42	-44.11	-6.50
Ba	45.98	109.63	-16.32	-14.50	11.46
Sn	41.07			-23.77	



TABLE IV. ALKALINE-EARTH MOH<sup>+</sup> KINETICS

i) M: Ca, Sr, Ba



$$[\Delta H_{298}(\text{kcal/mol}) = 36.05(\text{Ca}), 28.16(\text{Sr}), 12.63(\text{Ba})]$$

$$d[MOH^+]/dt = k[M][OH]$$

$$\sim [H]^3 \exp(-\Delta H_{298}/RT)$$

$$\sim 1.2 \times 10^{-4} [H]^3, \text{ Ca}$$

$$\sim 8.4 \times 10^{-4} [H]^3, \text{ Sr}$$

$$\sim 4.2 \times 10^{-2} [H]^3, \text{ Ba}$$

$$T = 2000 \text{ K}$$

TABLE V. SOOT REDUCTION CORRELATION WITH IONIZATION POTENTIAL

Metal	Flame species		IP(eV)	$f_v/f_v^0$
	Neutral	Charged		
Cu	Cu	$\text{Cu}^+$	7.72	1.03
Sn	SnO	$\text{Sn}^+$	7.33	1.00
Ca	Ca, CaO, CaOH	$\text{CaOH}^+$	5.55	1.00
Li	LiOH	$\text{Li}^+$	5.39	0.96
Na	Na	$\text{Na}^+$	5.14	0.52
Sr	Sr, SrO, SrOH	$\text{SrOH}^+$	5.10	0.27
Ba	Ba, BaO, BaOH	$\text{BaOH}^+$	4.35	0.10
K	K	$\text{K}^+$	4.34	~0.1

$$N(\text{Na}^+)/N(\text{Li}^+) \sim 4 (@2000 \text{ K})$$

TABLE VI. APPLICABILITY OF LIF TO ALKALINE-EARTH SPECIES DETECTION

	<u>Ca</u>	<u>Sr</u>	<u>Ba</u>
M	3)	3)	3)
MO	+	+	+
MOH	4)?, 5)	4), 5)	4)?, 5)
M(OH) <sub>2</sub>	2), 5)	2), 5)	2), 5)
M <sup>+</sup>	+	+	+
MOH <sup>+</sup>	1)	1)	1)

+ Meets criteria for detection in sooting flame

- 1) Spectra unknown
- 2) Spectra poorly known
- 3) Soot interference (Mie scattering)
- 4) Soot interference (laser modulated particulate incandescence)
- 5) Insufficient spectral resolution, unknown transition strengths, etc.

# FIGURE CAPTIONS

- Figure 1. Schematic diagram of apparatus: A, aperture; B, burner; BS, beam splitter; DP, dove prism; F, narrow-band optical filter; G, glass plate; L1, L2 and L3, plano-convex lenses; M1 and M2, partially reflecting mirrors; NDF, neutral density filter; P, polarization analyzing filter; PBP, Pellin-Broca prism; PMT, photomultiplier; T, light trap.
- Figure 2. End view of diffusion flame: a) no additive; b) 1.0 molar  $\text{BaCl}_2 \cdot 2\text{H}_2\text{O}$  additive
- Figure 3. Lateral profiles of flame temperature measured via the sodium line reversal method. Measurement height:  $\Delta$ , 8 mm;  $\circ$ , 18 mm;  $\nabla$ , 28 mm;  $\square$ , 38 mm.
- Figure 4a. Additive effectiveness on soot diameter. Measurement height: 23 mm.  $D^\circ$ : diameter with no additive.  $D$ : diameter with 0.2 molar  $\text{SrCl}_2 \cdot 6\text{H}_2\text{O}$  additive.
- Figure 4b. Additive effectiveness on soot number density. Measurement height: 23 mm.  $N^\circ$  = number density with no additive.  $N$ : number density with 0.2 molar  $\text{SrCl}_2 \cdot 6\text{H}_2\text{O}$  additive.
- Figure 4c. Additive effectiveness on soot volume fraction. Measurement height: 23 mm.  $f_v^\circ$ : volume fraction with no additive.  $f_v$ : volume fraction with 0.2 molar  $\text{SrCl}_2 \cdot 6\text{H}_2\text{O}$  additive.
- Figure 5. Lateral dependence of additive effectiveness on soot volume fraction for dissimilar metals. Measurement height: 23 mm. Additive molarity: 0.1.
- Figure 6. Additive effectiveness on soot volume fraction as a function of vertical distance above the center of the fuel slot. Lateral measurement position:  $x = 0$  mm. Additive: 0.1 molar  $\text{BaCl}_2 \cdot 2\text{H}_2\text{O}$ .
- Figure 7. Ba and BaO observed for flame seeded as in Fig. 2b above. The numerals in parentheses identify initial and final vibrational states for optical emission bands belonging to the  $A^1\Sigma + X^1\Sigma$  BaO system.
- Figure 8. Laser excited fluorescence of SrOH as a function of lateral position. Measurement height: 13 mm. Additive: 0.2 molar  $\text{SrCl}_2 \cdot 6\text{H}_2\text{O}$ .

Figure 9. Fluorescence intensity of SrOH as a function of laser energy at two different measurement positions. Point "A":  $x = 3.5$ ,  $z = 13$  mm. Point "B":  $x = 0$ ,  $z = 13$  mm. Additive: 0.2 molar  $\text{SrCl}_2 \cdot 6\text{H}_2\text{O}$ .

Figure 10. Lateral variation of  $[\text{H}]/[\text{H}_2\text{O}]$  concentration at  $z = 18$  mm measurement height.

FIG. 1

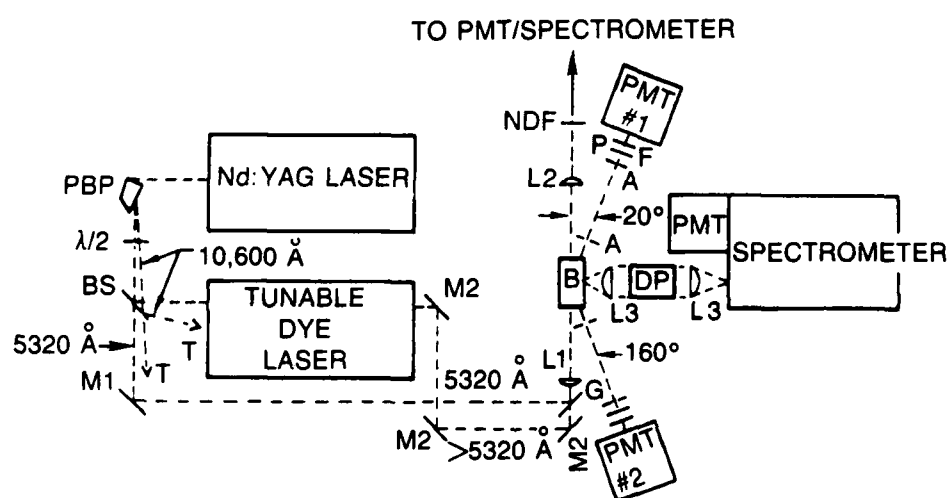


FIG. 2

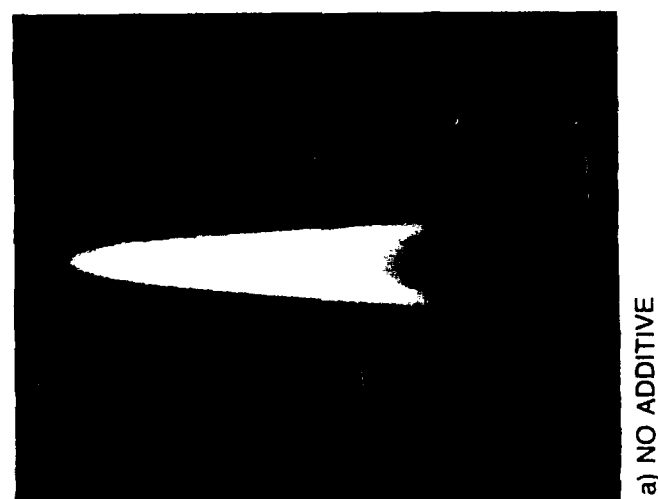


FIG. 3

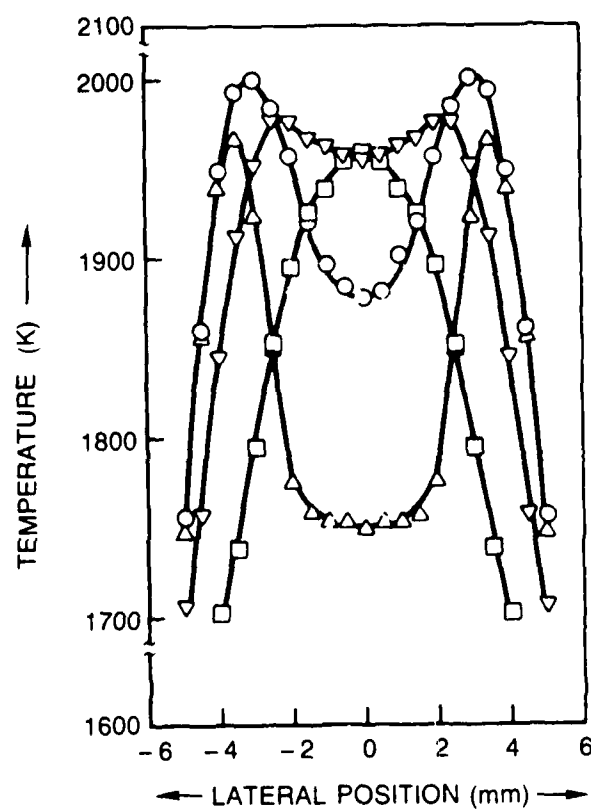




FIG. 4a

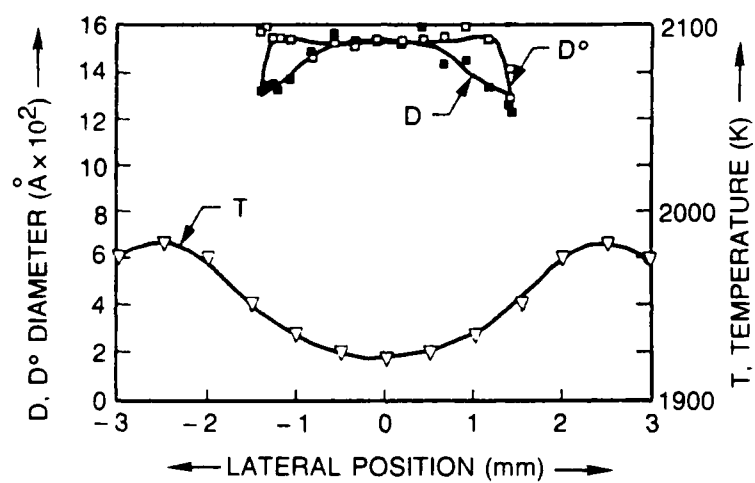
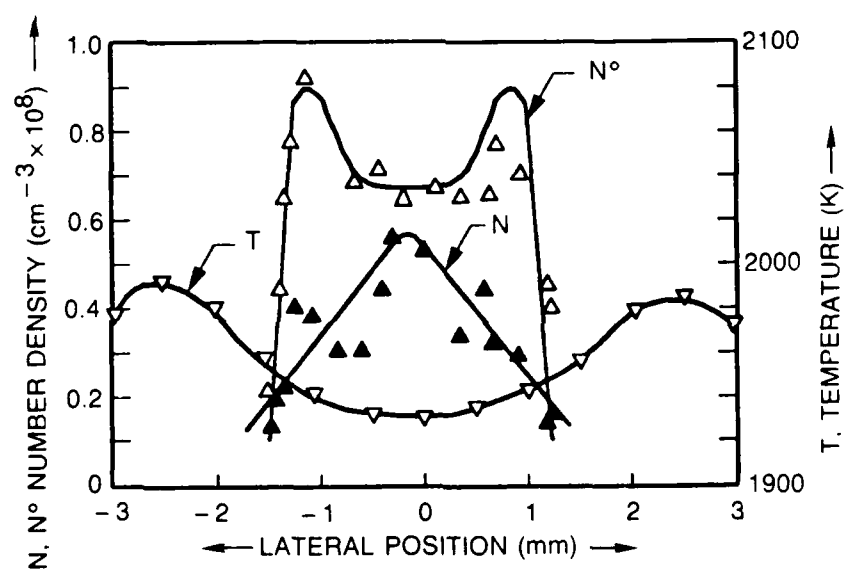


FIG. 4b



AD-A172 522 INVESTIGATION OF FUEL ADDITIVE EFFECTS ON SOOTING 2/2  
FLAMES(U) UNITED TECHNOLOGIES RESEARCH CENTER EAST  
HARTFORD CT P A BOMCZYK 31 JUL 86 UTRC/R06-936345-F  
UNCLASSIFIED AFOSR-TR-86-0051 F49620-83-C-0113 F/G 21/4 NL

INVESTIGATION OF FUEL ADDITIVE EFFECTS ON SOOTING  
FLAMES(U) UNITED TECHNOLOGIES RESEARCH CENTER EAST  
HARTFORD CT P A BOMBCHYK 31 JUL 86 UTRC/R86-95645-F  
AFOSR-TR-86-0854 F49620-83-C-0113 F/B 21/4

242

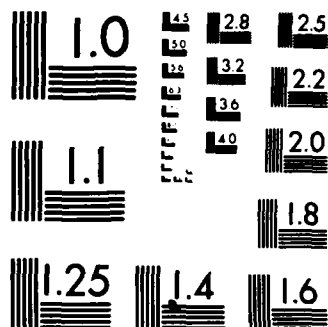
UNCLASSIFIED

AFOSR-TR-86-0851 F49620-83-C-0113

F/G 21/4

NL





MICROCOPY RESOLUTION TEST CHART  
NATIONAL BUREAU OF STANDARDS 1963-A

FIG. 4c

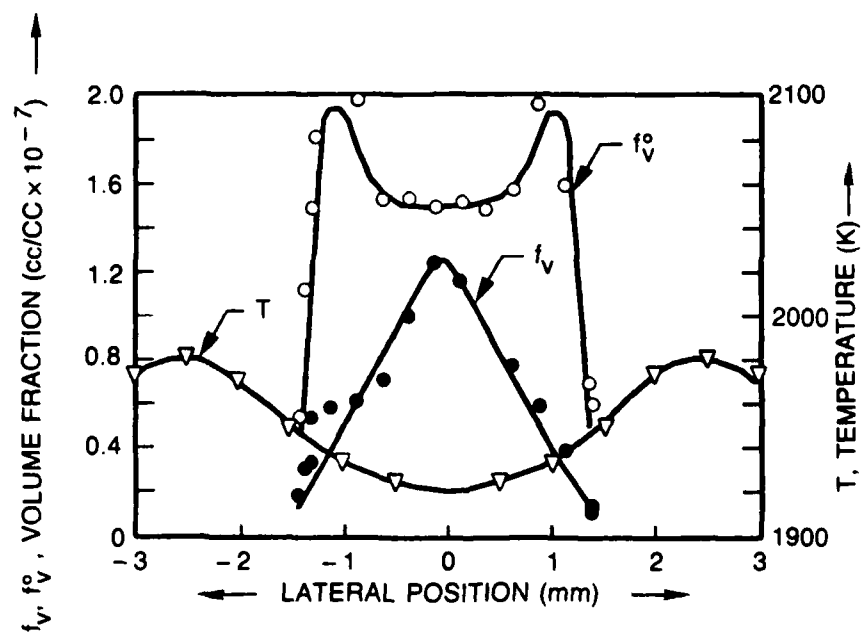


FIG. 5

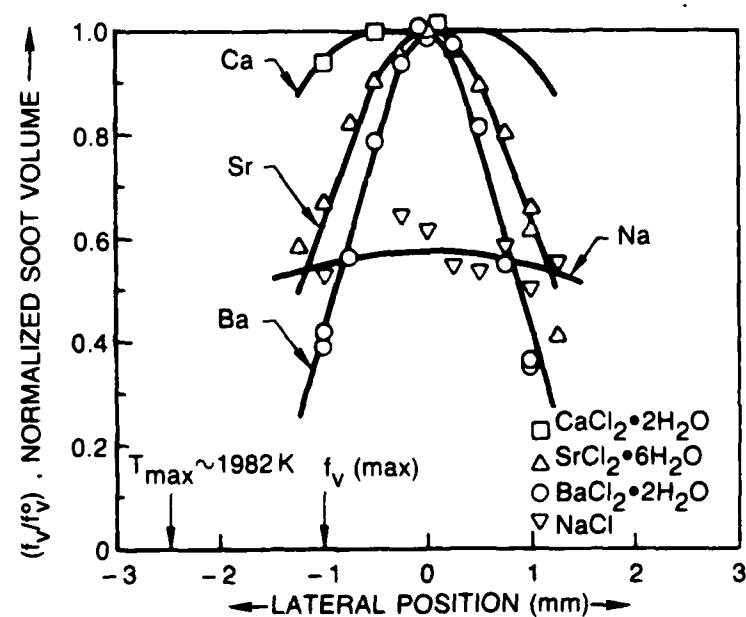


FIG. 6

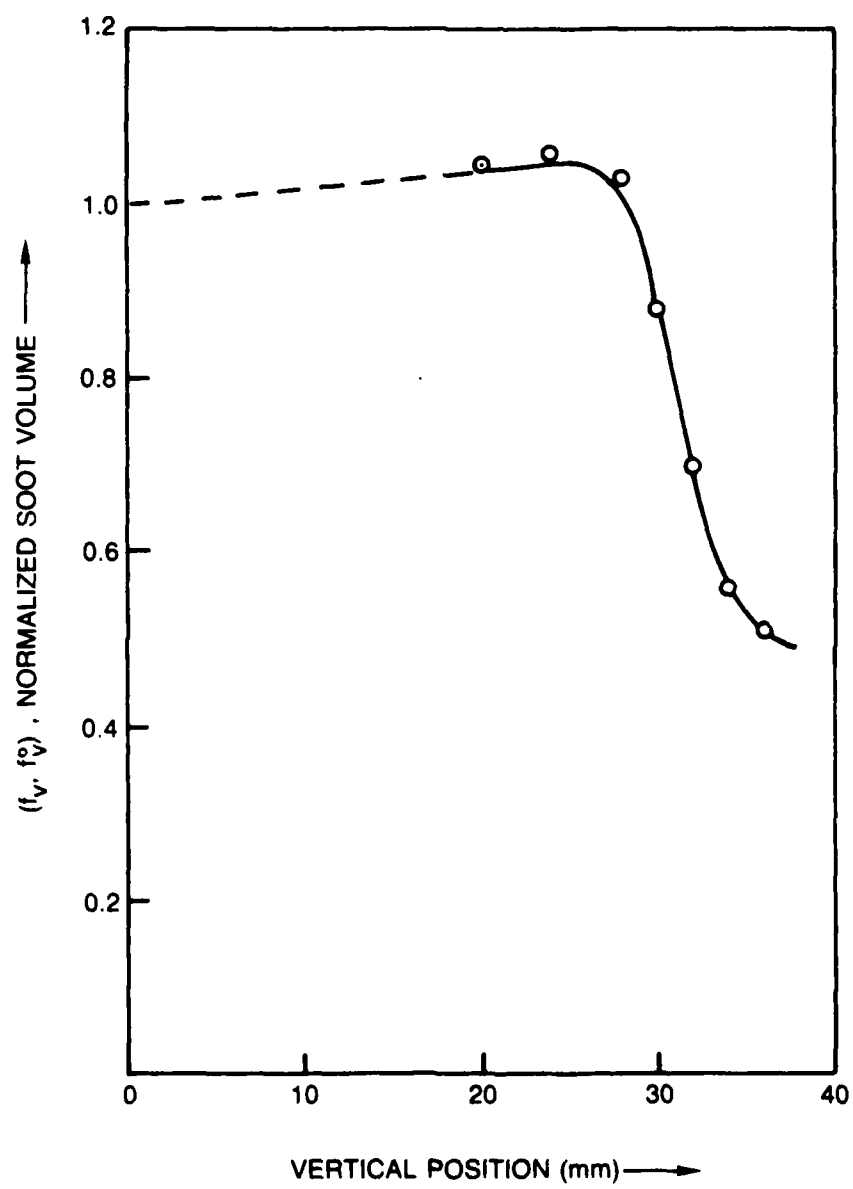


FIG. 7

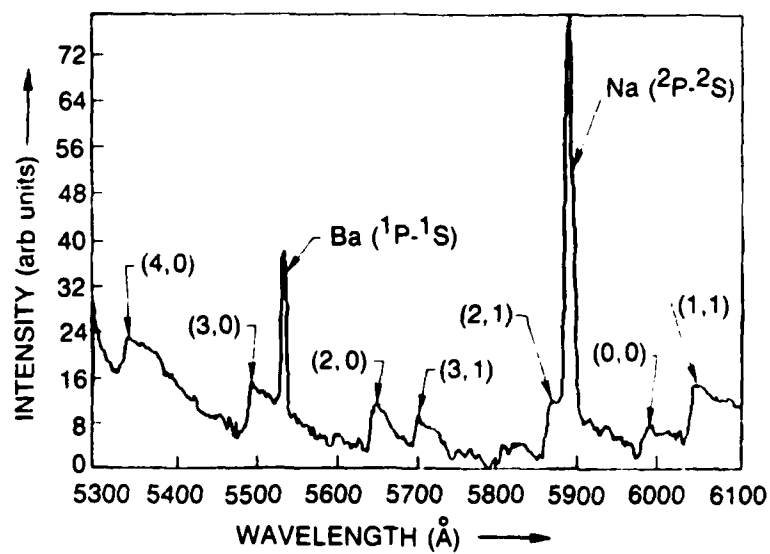




FIG. 8

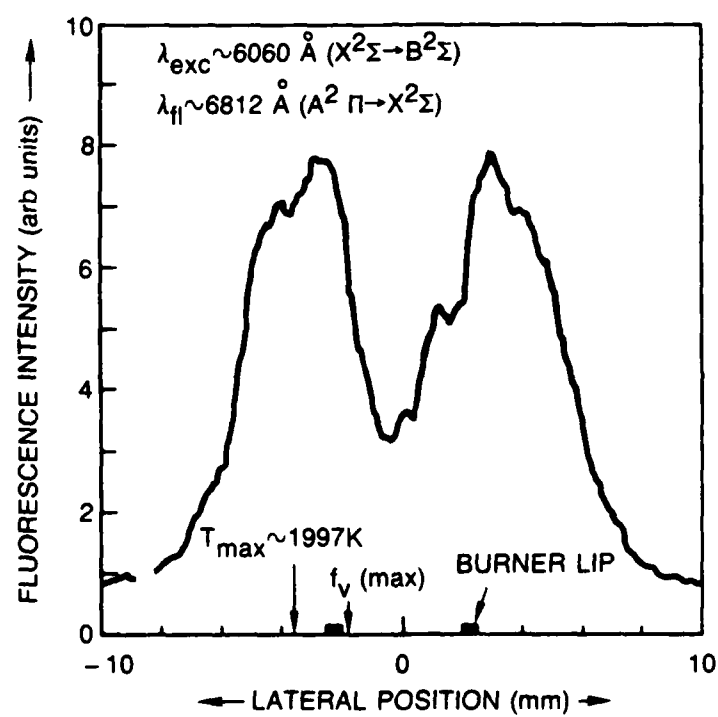


FIG. 9

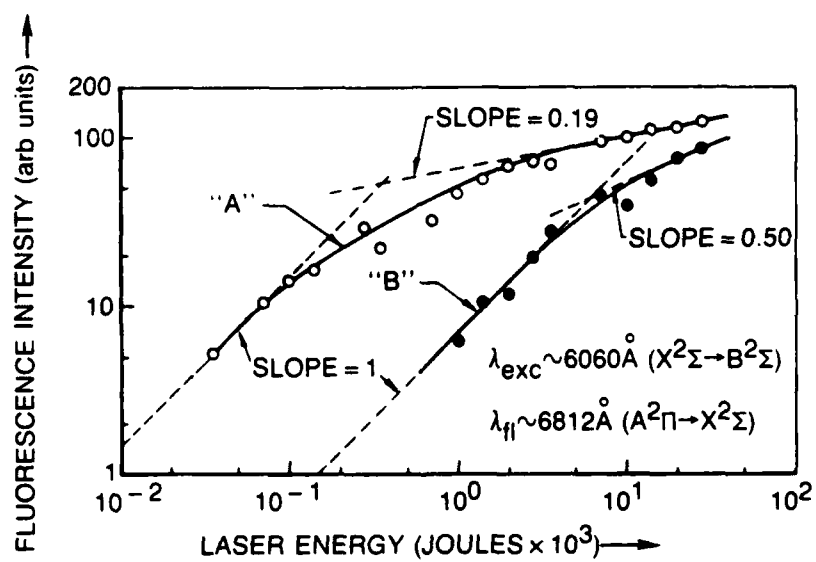
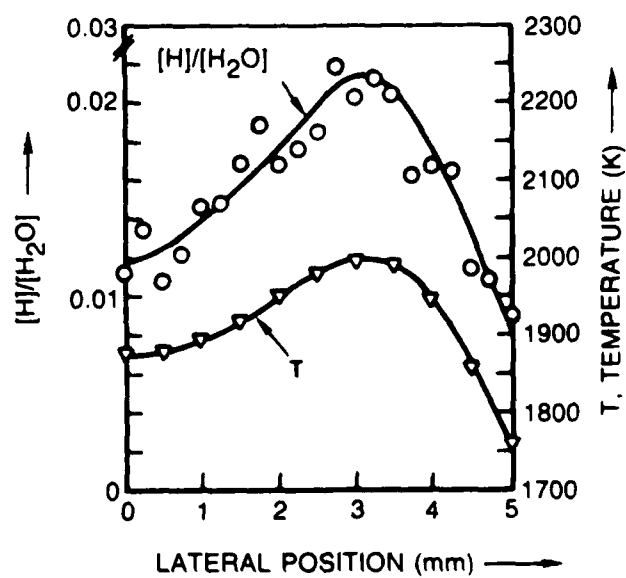


FIG. 10





**UNITED  
TECHNOLOGIES  
RESEARCH  
CENTER**

East Hartford Connecticut 06108

APPENDIX II

THE INFLUENCE OF ALKALINE-EARTH ADDITIVES ON SOOT AND HYDROXYL  
RADICALS IN DIFFUSION FLAMES\*

P. A. Bonczyk  
United Technologies Research Center  
East Hartford, Connecticut 06108

Submitted for Publication  
in COMBUSTION SCIENCE and TECHNOLOGY  
July, 1986

\*Jointly sponsored by the Air Force Office of Scientific Research (AFOSR) and the Environics Division of the Air Force Engineering Services Center (Tyndall AFB, Fla.) under AFOSR Contract F49620-83-C-0113.

# The Influence of Alkaline-Earth Additives on Soot and Hydroxyl Radicals in Diffusion Flames

P. A. Bonczyk  
United Technologies Research Center  
East Hartford, Connecticut 06108

When alkaline-earth metals are present as additives in flames, a significant reduction in the soot volume fraction occurs. This has been observed in laboratory-scale diffusion [1-3] and premixed [4] flames, as well as in practical combustion media [5-6]. There have been repeated speculations in the published literature concerning a possible chemical/OH explanation of alkaline-earth metal behavior in relation to soot [1-4, 7]. The soot reduction is presumed to occur via a metal-induced catalytic increase in OH, which then in turn increases the rate of soot (carbon) oxidative burn out given by,  $C_{\text{solid}} + OH + CO + (1/2) H_2$ . This communication describes the first quantitative test of this mechanism. The results which are presented below do not support it as a viable explanation of soot suppression by alkaline-earth metals.

## EXPERIMENT

Spatially-precise nonperturbing laser/optical techniques have been used to measure flame temperature and the effect of alkaline-earth salt additives on soot and OH in the luminous, sooting  $C_2H_4$ /air diffusion flame shown in Fig. 1. The flame emanates from a Wolfhard-Parker burner having a central 5 x 45 mm fuel slot, two adjacent symmetrically positioned 10 x 45 mm air (oxidant) slots, and

a surrounding flow of shroud air [8]. The fuel and oxidant flows are such that the flame is highly overventilated and, hence, the two flame sheets have a common apex. Metal salts are introduced into the flame by first dissolving them in water, and then aspirating the solution into the two oxidant slots using a pneumatically operated nebulizer (Varian Type 99-100236-00). The oxidant flow to the flame and the air flow to actuate the nebulizer are one and the same. Due to rapid diffusion, this method of insertion results in uniform dispersal of the metal transverse to the direction of flow at a 13 mm height and above. This was verified from optical absorption measurements of sodium atom concentrations.

Soot size, number density and volume fraction are inferred from particulate/Mie scattering of 532 nm, pulsed Nd:YAG laser radiation [9, 10]. In the Mie analysis, particulate nonsphericity is neglected, a monodisperse size distribution is assumed, and the refractive index is taken as known. The soot mean diameter,  $D$ , is evaluated from the  $20/160^\circ$  ratio of scattered light intensities. Having  $D$ , the number density,  $N$ , is obtained from the absolute scattered intensity at either angle. Then, the volume fraction,  $f_v$ , is calculated from,  $f_v = (\pi D^3/6)N$ .

The OH concentrations were inferred from saturated laser-induced fluorescence measurements [10, 11]. The exciting light near 309 nm was obtained by frequency doubling the output of a dye laser pumped by the 532 nm laser mentioned above. Fluorescence was observed at 90-degrees to the direction of the exciting light. There, a narrow band spectrometer, centered near 312 nm, was used to measure fluorescence and to avoid intense, interfering Mie signals at 309 nm. In

order to arrive at absolute OH concentration values, the fluorescence measurements were supplemented by Rayleigh calibration of the light collecting optics [12]. The Rayleigh measurements were made with the flame extinguished and the spectrometer tuned to the 309 nm laser wavelength.

## RESULTS

Measurements were made of the effect of additives of the type  $XCl_2 \cdot nH_2O$  ( $X = Ca, Sr$  and  $Ba$ ) on the soot parameters  $D$ ,  $N$  and  $f_v$ . Ancillary tests showed that additive effectiveness was insensitive to the chemical nature of the salts anion. Accordingly, chlorides of the alkaline-earth metals were selected since their water solubilities are high, thereby permitting optimum total metal species concentrations in the flame. These were, roughly,  $10^{12} \text{ cm}^{-3}$  for a (2/10) molar solution. Additive effectiveness in suppressing soot was measured from point-to-point throughout the flame. The spatial precision was  $10^{-2} \text{ cm}$  in the plane of Fig. 1a and roughly (1/2) cm orthogonally to it. Generally, additive effectiveness was strongly position dependent, tending to maximize near both the flame tip and the main reaction zone. An example of this behavior is shown in Fig. 2 where additive effect on volume fraction is determined for fixed vertical and variable lateral measurement positions. Measurements were made for three different metals, with  $Ba > Sr > Ca$  as concerns soot removal efficiency. Further, for both  $Ba$  and  $Sr$ , effectiveness is a minimum at the burner center and, as is apparent in Figs. 3 and 4a below, increases in the direction of increasing temperature and OH concentration. Other data not included here show that  $f_v^\circ$  reduction occurs due to decreases in both  $N^\circ$  and  $D^\circ$ , but not quite in the same way for  $Ba$  and  $Sr$ . For

example, at +1 mm in Fig. 2, the effect of Ba (Sr) on soot is:  $f_v/f_v^\circ = 0.36$  (0.62);  $N/N^\circ = 0.68$  (0.69);  $D/D^\circ = 0.81$  (0.96). Accordingly, for Ba a reduction in  $N^\circ$  and  $D^\circ$  occurs, whereas for Sr the change in  $D^\circ$  is nearly imperceptible.

The lateral dependence of OH concentration at a 23 mm measurement height is shown in Fig. 4a. The OH concentrations were inferred from  $P_1(8)$  fluorescence intensities at 311.8 nm following  $Q_1(7)$  excitation at 309.0 nm. Both excitation and fluorescence involved single rotational levels in the OH ( $X^2\Pi, v'' = 0 + A^2\Sigma, v' = 0$ ) spectrum [13], and nearly complete saturation of the fluorescence emission was observed. The relative lateral positions of the soot, temperature and OH peaks in Figs. 2, 3 and 4a are similar to those observed previously in  $C_2H_4/O_2$  [14] and  $CH_4/air$  [15] diffusion flames. In particular, the soot and OH peaks are well removed from one another [14, 15]. The OH radicals were observed throughout the flame in Fig. 1, with concentration variations resembling the temperature profiles in Fig. 3. The effect of alkaline-earth metal additives on OH is shown in Fig. 4b. There the additive is seen to reduce the OH concentration to a degree dependent upon the particular metal selected and the lateral measurement position in the flame. Significantly, there is, therefore, no evidence of additive enhancement of OH concentration and consequent more rapid soot oxidative burnout as previously has been suggested [1-4, 7]. Data similar to those in Fig. 4b were obtained at other vertical positions as well; hence, there was no additive enhancement of OH at any point in the flame.



## DISCUSSION

The metal-induced decrease in  $[\text{OH}]$  reported here has a similar precedent. For example, in fuel-rich premixed  $\text{H}_2/\text{O}_2/\text{N}_2$  flames the rate of recombination of H-atoms is accelerated by the addition of alkaline-earth metals [16], and as in Fig. 4b,  $\text{Ba} > \text{Sr} > \text{Ca}$  describes the relative catalytic efficiencies of the metals. In addition, for any one metal the catalytic efficiency increases with decreasing temperature or increasing distance from the main reaction zone [16]. For Ba, for example, the decrease in  $[\text{H}]$  results from the reaction sequence 1)  $\text{BaO} + \text{H}_2\text{O} \rightarrow \text{Ba}(\text{OH})_2$ , 2)  $\text{Ba}(\text{OH})_2 + \text{H} \rightarrow \text{BaOH} + \text{H}_2\text{O}$  and 3)  $\text{BaOH} + \text{H} \rightarrow \text{BaO} + \text{H}_2$  [17], which effectively accelerates the recombination  $\text{H} + \text{H} \rightarrow \text{H}_2$ . Since  $[\text{H}]$  and  $[\text{OH}]$  are linked at any point by the balanced reaction  $\text{H}_2\text{O} + \text{H} \rightleftharpoons \text{H}_2 + \text{OH}$ , and since  $[\text{H}_2\text{O}]$  and  $[\text{H}_2]$  are essentially constant, a decrease in  $[\text{H}]$  is accompanied by a  $[\text{OH}]$  decrease as well. Accordingly, a related action of the metal, as evident in Fig. 4b, is to accelerate the recombination  $\text{H} + \text{OH} \rightarrow \text{H}_2\text{O}$  as well. In general, metals may increase radical concentrations by stimulating the dissociation of  $\text{H}_2$  and/or  $\text{H}_2\text{O}$ . This occurs when the radical concentrations are significantly below their equilibrium values. The further significance, then, of Fig. 4b is that  $[\text{OH}]$  in the sooting,  $\text{C}_2\text{H}_2/\text{air}$  flame is at or significantly above its equilibrium value despite the presumed presence of OH removal via its oxidative reactions with soot and/or soot precursors.

The  $[\text{OH}]$  decrease above has been ascribed to metal enhanced radical recombination. However,  $[\text{OH}]$  is sensitive to temperature changes as well, which in principle may occur when seeding the flame with metallic salts. In order to rule

out the latter as responsible for the data in Fig. 4b, flame temperatures with and without (1/10) molar  $\text{BaCl}_2 \cdot 2\text{H}_2\text{O}$  seeding were determined by a method based on the ratios of OH emission intensities [18]. The measurement gave a roughly (20-40)K temperature increase with seeding, which agrees with a similar observation by others [4]. The increase is due to reduced radiative cooling of the flame, which results from additive removal of soot. Since [OH] increases with increasing temperature, the latter effect is not responsible for the [OH] decrease in Fig. 4b.

Strong suppression of soot by alkaline-earth additives is evident in Fig. 2. A frequently cited chemical/OH explanation of this behavior has been shown above to be inaccurate. On the other hand, in closely related work evidence has been compiled by us for an electrical mechanism in which  $\text{MOH}^+$  ( $\text{M} = \text{Ba}, \text{Sr}, \text{Ca}$ ) are the active species. This result is consistent with our earlier alkali metal additive work in which metal cations were critical as well [9]. Discussion of the electrical mechanism and the supporting evidence for it is beyond the scope of this brief communication and, hence, the details will be presented elsewhere [19].

#### ACKNOWLEDGEMENT

This research was jointly sponsored by the Air Force Office of Scientific Research (AFOSR) and the Environics Division of the Air Force Engineering Services Center (Tyndall AFB, Fla.) under AFOSR Contract F49620-83-C-0113.

## REFERENCES

1. Cotton, D. H., Friswell, N. J., and Jenkins, D. R., *Combust. Flame* 17: 87-98 (1971).
2. Bulewicz, E. M., Evans, D. G., and Padley, P. J., 15th Symposium (International) on Combustion, The Combustion Institute, 1974, pp. 1461-1470.
3. Ndubizu, C. C., and Zinn, B. T., *Combust. Flame* 46:301-314 (1982).
4. Haynes, B. S., Jander, H., and Wagner, H. Gg., 17th Symposium (International) on Combustion, The Combustion Institute, 1979, pp. 1365-1374.
5. Shayeson, M. W., *SAE Transactions* 76:2687-2694 (1968).
6. Friswell, N. J., in Emissions from Continuous Combustion Systems (W. Cornelius and W. G. Agnew, Eds.), Plenum Press, New York, 1972, pp. 161-182.
7. Feugier, A., *Adv. Chem. Ser.* 166 (Evaporation-Combust. Fuels): 178-189 (1978).
8. Kent, J. H., and Wagner, H. Gg., *Combust. Flame* 47:53-65 (1982).
9. Bonczyk, P. A., *Combust. Flame* 51:219-229 (1983).
10. Bonczyk, P. A., in Analytical Laser Spectroscopy (S. Martellucci and A. N. Chester, Eds.), Plenum Press, New York, 1985, pp. 107-130.
11. Lucht, R. P., Sweeney, D. W., and Laurendeau, N. M., *Combust. Sci. Tech.* 42:259-281 (1985).
12. Salmon, J. T., and Laurendeau, N. M., *Appl. Opt.* 24:65-73 (1985).
13. Lucht, R. P., Sweeney, D. W., and Laurendeau, N. M., *Appl. Opt.* 19:3295-3300 (1980).
14. Wolfhard, H. G., and Parker, W. G., *Proc. Phys. Soc.* 65A:2-19 (1952).
15. Smyth, K. C., Miller, J. H., Dorfman, R. C., Mallard, W. G., and Santoro, R. J., *Combust. Flame* 62:157-181 (1985).
16. Cotton, D. H., and Jenkins, D. R., *Trans. Faraday Soc.* 67:730-739 (1971).
17. Jensen, D. E., and Jones, G. A., *Proc. R. Soc. Lond.* A364:509-535 (1978).
18. Vaidya, D. B., Horvath, J. J., and Green, A. E. S., *Appl. Opt.* 21:3357-3362 (1982).
19. Bonczyk, P. A. (to be published).

# FIGURE CAPTIONS

- Figure 1. End (a) and side (b) views of  $C_2H_4$ /air diffusion flame.
- Figure 2. Lateral dependence of soot volume fraction with (1/10) molar ( $=f_v$ ) and with "zero" molar ( $=f_v^0$ ) additive salt seeding. Measurement height: 23 mm. Additive salt :  $\Delta$ ,  $CaCl_2 \cdot 2H_2O$ ;  $\square$ ,  $SrCl_2 \cdot 6H_2O$ ;  $\circ$ ,  $BaCl_2 \cdot 2H_2O$ .
- Figure 3. Spatial profiles of flame temperature measured via the sodium line reversal method. Measurement height:  $\Delta$ , 13 mm;  $\circ$ , 23 mm;  $\square$ , 33 mm.
- Figure 4a. Lateral dependence of OH concentration without additives present ( $=N_{OH}^0$ ). Measurement height: 23 mm.
- Figure 4b. Lateral dependence of the ratio of OH concentrations with (1/10) molar ( $=N_{OH}$ ) and with "zero" molar ( $=N_{OH}^0$ ) additive salt seeding. Measurement height: 23 mm. Additive salt:  $\Delta$ ,  $CaCl_2 \cdot 2H_2O$ ;  $\square$ ,  $SrCl_2 \cdot 6H_2O$ ;  $\circ$ ,  $BaCl_2 \cdot 2H_2O$ .

FIG. 1

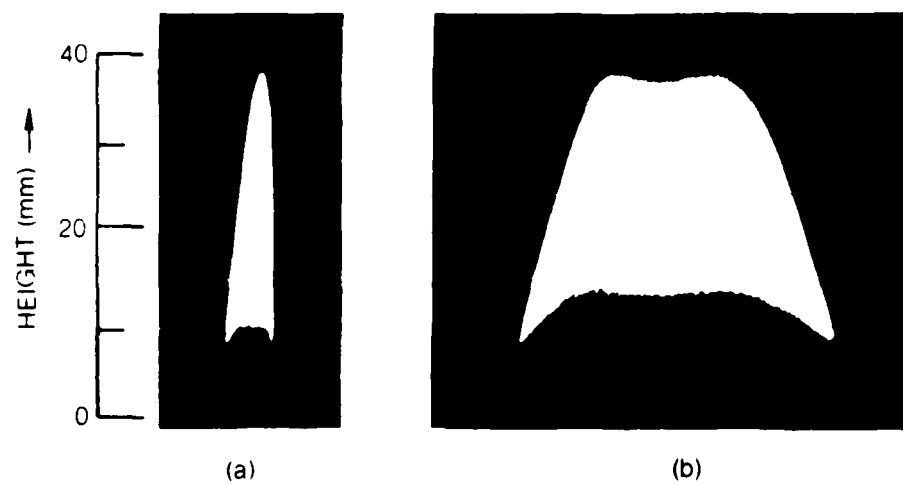


FIG. 2

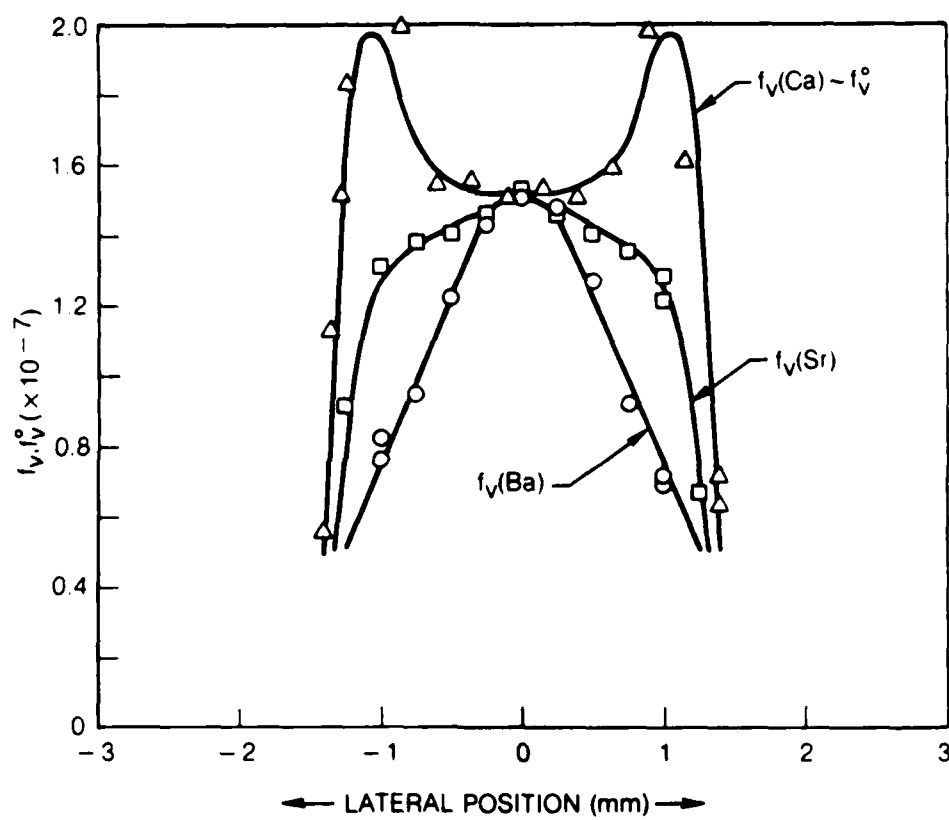


FIG 3

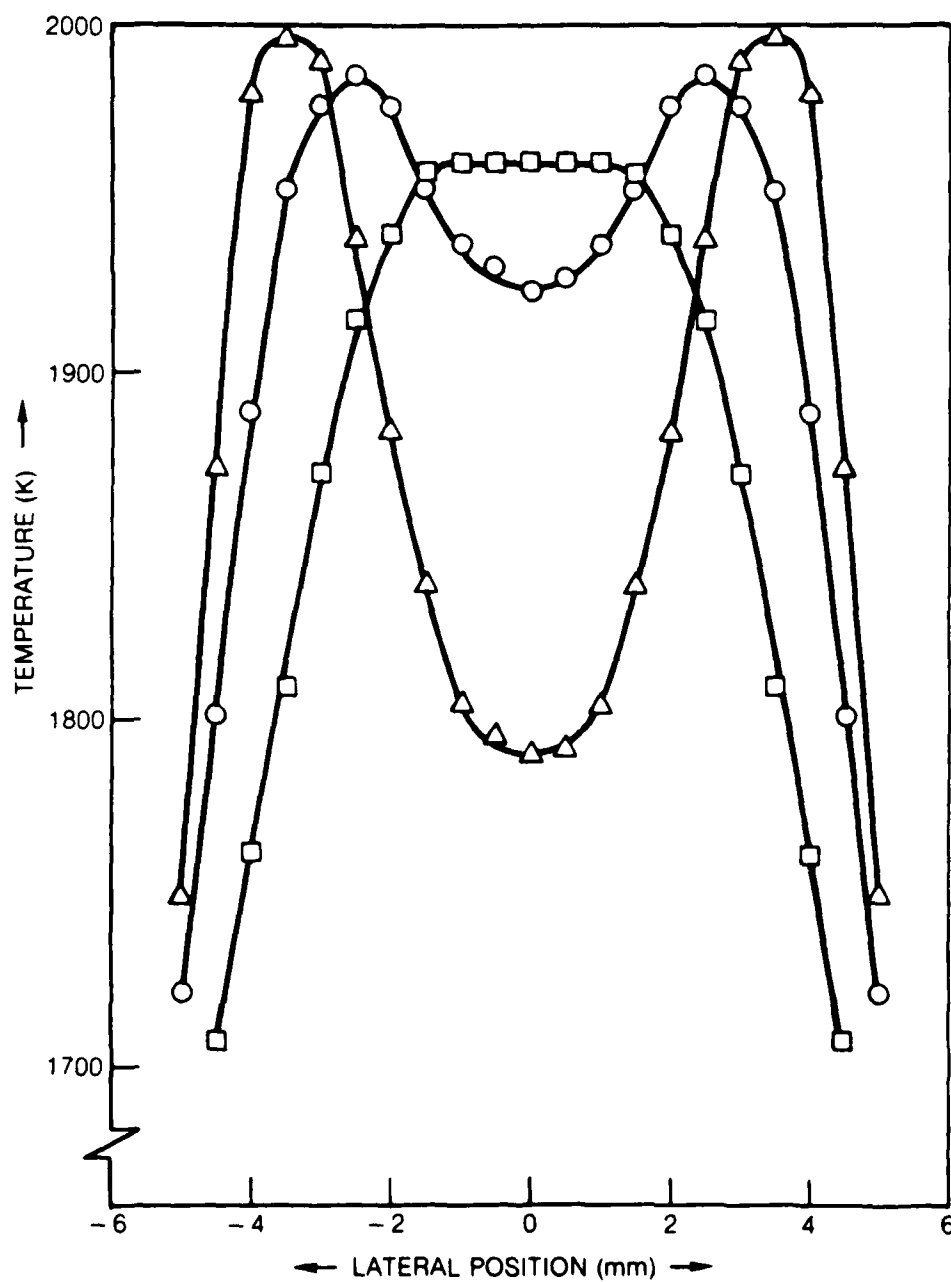


FIG 4a

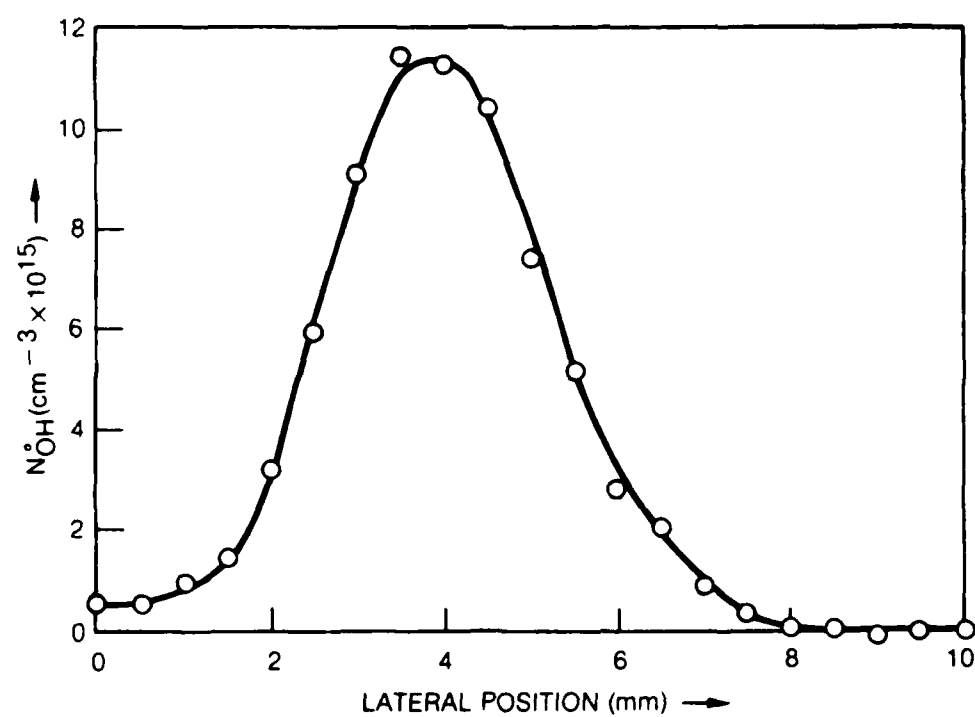
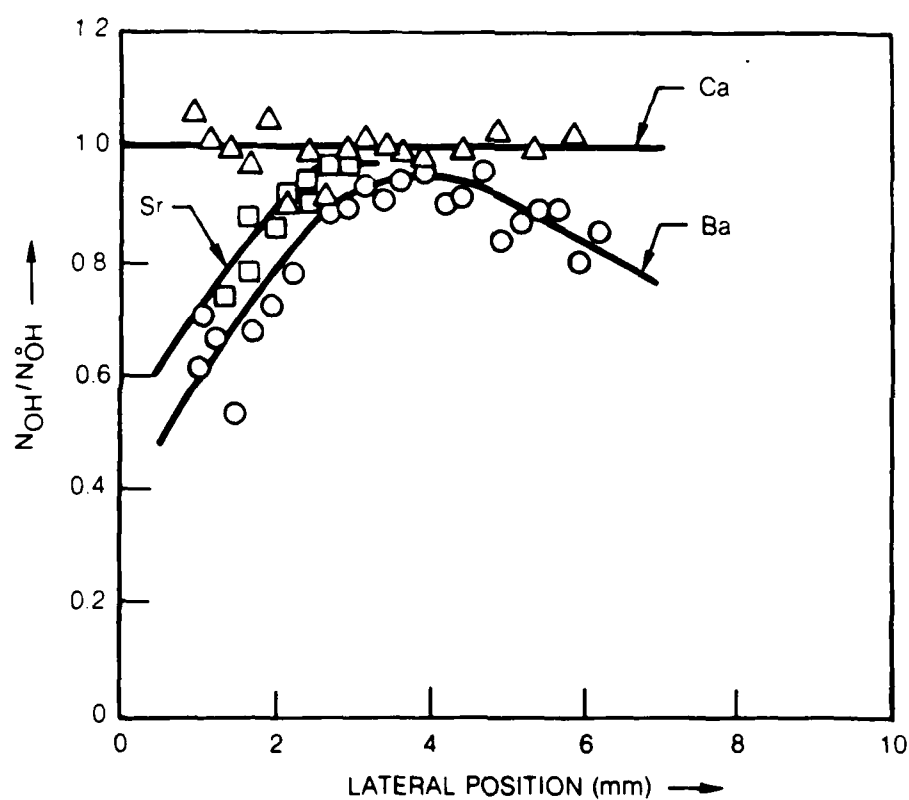




FIG. 4b



## APPENDIX III

### Additive Effects on Soot in Prevaporized Liquid-Fueled Flames\*

Laurence R. Boedeker and Paul A. Bonczyk  
United Technologies Research Center  
East Hartford, CT 06108

#### INTRODUCTION

The Chemical Physics Group at UTRC was requested by the Advanced Projects Group at the Government Products Division of Pratt and Whitney in West Palm Beach, Florida to perform tests to determine the sooting characteristics of a laboratory flame burning JP4 and toluene fuels with ferrocene and cerium based smoke suppressant additives (Refs. 1, 2). As a consequence, a program was conducted at UTRC during early 1985 to complete the development of a laboratory, prevaporized-liquid-fuel burner to study techniques to introduce the suppressants into the flame in a homogeneous fashion, and to determine the overall smoke-point characteristics of the various flames. The results of this program are presented in the following sections of this report. It was originally thought that experimental measurements of soot properties would be necessary using laser light scattering. However, progress with smoke-point type measurements was substantial and moreover showed that very extensive laser probing was not required. The experiments focused more on overall soot reduction and elimination with additives as evidenced by a quantitative smoke-point fuel flowrate comparison.

#### PREVAPORIZED FUEL BURNER

A prevaporized-fuel axisymmetric diffusion flame burner had been developed at UTRC in the previous year for use with relatively low sooting liquid fuels. Fuel flow rate is controlled with this burner by a positive displacement liquid micro-pump. This burner has been applied here to the study of soot suppression by additives for highly sooting liquid fuels. The controlled fuel flow rates that are possible with this burner result in more quantitative and comparative data on soot suppression by additives than are possible with a wick flame approach (Ref. 3). For present purposes it was necessary to modify and check out the burner, the liquid fuel delivery system, and the post-flame soot handling system for liquid fuels. These are highly sooting and require careful control of conditions with low fuel flow rates. The resultant overall system is shown in Fig. 1. The burner fuel tube has an inside diameter,  $d = 10.8$  mm. It is isolated from the air plenum by air gaps using a thin shell support structure. A thin cartridge heater heats the top portion of the burner tube directly through

---

\*Supported by Government Products Division, United Technologies Corporation

an intermediate, slip-fit, slotted plug. The cartridge heater and its leads are isolated from the hot fuel vapor and the leads are brought out through a feed-through at the bottom of the burner tube. A band heater is used to heat the base of the fuel tube through an intermediate thick metal ring clamped to the fuel tube. A small vaporizer is provided for the low flow rates employed in order to avoid excessively long flame adjustment times. The burner tube thermal isolation is adequate enough so that temperature with the flame on can be adjusted up to about 250 C at all points along the vaporizer and burner tube, sufficient to sustain essentially complete vaporization of JP4 and provide an excess fuel preheat capability of about 150 C for toluene. A bypass system is provided for the fuel, using a 3-way micro-valve, in order to switch fuels in a reasonable time. The positive displacement micro-pump was operated at high flow rate in the bypass mode when switching to a different fuel, and then at the desired low flow rate during flame tests. A miniature, 6 port, rotary switch was added to facilitate comparative fuel/additive studies. In all cases here, the additives were dissolved in various concentrations in the fuel. The entire system was installed and checked out to achieve compatibility with the laser MIE scattering diagnostic. Since net soot escape from the flames could be high at times, it was necessary to completely confine the postflame gases, separate out large soot agglomerations, and prevent escape of soot into the room where it might contaminate optical and electronic equipment.

The air gap which exists between the fuel tube and the air smoothing honeycomb is maintained as the fuel tube passes through the air plenum, and is sealed against spurious thermal convection. The ferrocene added in tests to be described below vaporized with the fuel since a red ring, presumably iron oxide, formed on the burner lip.

#### CHARACTERISTICS OF TOLUENE DIFFUSION FLAMES WITH FERROCENE ADDITIVE

Toluene, as a monoaromatic, is known to be a highly sooting fuel (Ref. 4). The smoke-point for toluene in the present burner would correspond to an extremely small fuel mass flow rate and a smoke-point flame height less than the burner fuel tube diameter,  $d = 1.08$  cm. Large net smoke emission would occur for flow rates only a small amount larger and would be difficult to control with the present fuel delivery system. Instead a mixture of toluene with a less sooting liquid fuel, iso-octane (2,2,4 trimethylpentane), has been studied in order to deal with more reasonable flow rates and flame heights. Diluent nitrogen is added as a practical matter to avoid trapping fuel in upstream cold spots in the vaporizer and to also increase fuel flow rate at the smoke-point (Ref. 4). An additional benefit is that the larger flames are easier to include within a general temperature-soot correlation framework that is evolving through studies at UTRC (Ref. 5) and elsewhere. The toluene/iso-octane weight mixture ratio selected was 1/4, which is close to the proportions used in wick-flame studies at UTRC (Ref. 3). The flow rate of diluent nitrogen was fixed at about 37 sccm, which corresponds to a vapor transit time through the vaporizer and burner fuel tube of about 1 minute.

Ferrocene as a fuel additive is a known smoke suppressant. Here it is convenient to use ferrocene since it is highly soluble in toluene and other fuels, possesses a relatively high vapor pressure (Ref. 6) at typical temperatures required for vaporization of a toluene/iso-octane mixture ( $> 100\text{ C}$  at one atmosphere pressure), and the vaporized ferrocene molecule is stable. Accounting for dilution by nitrogen, it should be possible here to add up to about 0.3% by weight of ferrocene to the fuel and maintain effectiveness of vaporization.

An example of soot reduction with ferrocene added to a toluene/iso-octane flame in the prevaporized fuel burner is as follows. At a fixed fuel flow rate of 100 microliters/minute in the positive displacement pump, switching the fuel selector valve from a fuel reservoir without ferrocene to a reservoir with 0.3% ferrocene resulted in complete suppression of a large column of soot (net smoke) emerging from the flame. A ferrocene concentration of 0.1% was tried but did not suppress a visual soot breakthrough column. Fuel flow rate stability on average is well controlled by the precision components of the micropump. The average flow rate values have been checked over a period of 10-20 minutes by collecting the liquid in the by-pass mode in a small graduated cylinder. Some short term pulsations are present in flame height, likely due to fuel flow disturbances introduced as the pump stroke recycles rapidly, or to detailed dynamics of vaporization. All heater settings remained constant during the change of fuels, and the temperature distribution along the vaporizer and burner tube is expected to have remained the same for the two flames. Burner tube tip temperature was slightly above  $100\text{ C}$  with the flame on for these tests as checked with a thermocouple probe. The vaporizer and burner base temperature controllers were set at about  $200\text{ C}$  and the cartridge heater was not yet installed. The average height of the ferrocene flame above was about 29 mm. In subsequent repeatability tests the height of this flame was measured directly with a cathetometer and found on average to be 28 mm with a variation due to short term effects of about  $\pm 2\text{ mm}$ . These results at 100 microliters/minute are very similar to wick flame soot suppression effects noted in the prior studies (Ref. 3); however the wick flame fuel flow rate is essentially not known.

Control of fuel flow rate with the pre-heated burner was used to establish the smoke-point for the no additive toluene/iso-octane mixture. With constant burner heater settings and constant nitrogen diluent flow rate the positive displacement pump flow rate setting was gradually reduced until an average condition was identified for which soot breakthrough could just be observed. This corresponded to a fuel flow rate of 80 microliters/minute. Soot breakthrough occurred essentially from the tip of the flame. A very slight annular soot ring could be observed as weak soot wings on either side of the center tip. Addition of 0.3% ferrocene to the fuel again caused complete suppression of soot breakthrough and a wing structure was more evident. A ferrocene concentration of 0.1% was also found to suppress the smoke-point soot breakthrough. The boundary between soot breakthrough and soot suppression for ferrocene was identified here

by measuring the smoke-point fuel flow rates for ferrocene concentrations of 0.1 and 0.3%. For 0.1% ferrocene the smoke-point fuel flow rate increased to 90 microliters/minute and a slightly taller flame with more prominent soot wing features was evident. With 0.3% ferrocene, a doubling of fuel flow rate to 160 microliters/minute was required to reach a smoke-point. A much taller flame with prominent soot wing structure was observed. The effectiveness of ferrocene would appear to be higher with increasing ferrocene concentration in this comparison.

#### CERIUM ADDITIVE STUDIES

Cerium has presented some difficulties in introduction into the flame as a fuel additive with the pre-heated fuel burner. The commercial cerium compound that is typically added to fuel is very soluble in fuels such as toluene and JP4, but it does not appear to possess high volatility. No effect of this additive was noted in tests with the toluene/iso-octane fuel, when tested at 0.3 weight percent, probably because the cerium compound did not vaporize with the fuel. In a practical application the flames are fed with a liquid spray. In the basic studies here it would be very difficult to implement spray injection. As an alternative some research type cerium compounds were obtained which have higher volatility. These compounds however were found to be soluble in methanol but not in toluene or iso-octane. Methanol with dissolved cerium did not mix well with either JP4 or toluene. A further search for suitable cerium and solvent combinations is required.

#### STUDIES WITH JP4 FUEL

The boiling range of JP4 is about 100-250 C. In order to study this fuel with the pre-heated fuel burner (Fig. 1) it was necessary to increase the burner tube tip temperature above the level achieved in the above toluene/iso-octane tests. The brute-force approach would be to increase the band heater control temperature setting until 250 C was achieved at the tip. This would subject the JP4 to quite high temperatures at the base of the burner and spurious catalytic cracking or coking problems might be encountered. Instead, as discussed above, a heating section was added directly inside the burner tube as it passes through the air plenum to achieve more independent control of the burner tip temperature. This modification consists of a precision slotted stainless steel plug which encloses a 35 Watt 3.2 mm diameter cartridge heater on the inside and fits into a reamed surface on the I.D. of the nickel burner tube. The leads of the heater are enclosed within a 3.2 mm stainless steel hypo-tube and are led out through a fitting at the bottom of the burner tube. Since the percentage of aromatics in JP4 is not too different from the toluene/iso-octane mixture the smoke-point characteristics of a purely JP4 fueled flame here might not be too different from the toluene/iso-octane flame. Measurement experience to date with JP4 would appear to support this correlation. However, suppression of soot and increase of the smoke-point fuel flow rate was greater with ferrocene as an additive to JP4. Detailed measurement results are discussed below.

## OVERALL SMOKE-POINT COMPARISON

The smoke-point measurements were performed with JP4 for a burner exit temperature of about 250 C, achieved with the slotted plug cartridge heater at its maximum power of 35 Watts. The burner base heater was set at 280 C and the vaporizer at 260 C. Using the same heater settings the previous toluene/iso-octane results were repeated to study the effect of fuel preheat temperature in that case. Results and a comparison with the lower temperature toluene/iso-octane data are given in Table 1. Increase of the fuel pre-heat temperature is seen to have caused a slightly higher tendency for toluene/iso-octane to soot. In the case of JP4 ferrocene has a greater soot suppression capability, particularly at lower ferrocene concentrations. A ferrocene concentration of 0.1% increased the smoke-point fuel flow rate for toluene/iso-octane by only 20%, but for JP4 the increase was 90%.

## DISCUSSION AND RECOMMENDATIONS

The smoke-point results with ferrocene for the two fuels studies were all obtained under similar fuel preheat conditions and hence probably similar ferrocene concentrations were actually present in the flame environment. This may suggest that there is a fuel dependent process present here which might explain the greatly different sensitivity of the soot suppression to ferrocene concentration that exists between toluene/iso-octane and JP4. Temperature differences related to adiabatic flame temperature and flame structure must be evaluated in the two cases however, since temperature likely plays a role. As a practical matter the recommended ferrocene concentration for an actual application may depend on the detailed structure and blend of the fuel that is being used.

#### REFERENCES

1. Reilly, R. S., GPD Internal Correspondence, 7 December 1984.
2. Reed, H., GPD/UTRC Work Authorization, 17 December 1984.
3. Bonczyk, P. Measurements of Metallic Fuel Additive Effects on Soot in Diffusion Flames. 20th Symposium (International) on Combustion, Poster Paper PS29, August 1984.
4. Gomez, A., Sidebotham, G., and Glassman, I. (1984). Sooting Behavior in Temperature-controlled Laminar Diffusion Flames. Combust. Flame, 58, 45.
5. Boedeker, Laurence R., and Dobbs, Gregory M., (1985). CARS Temperature Measurements in Sooting, Laminar Diffusion Flames. Combust. Flame, to be published.
6. Jacobs, M. H. G., et al. (1983). The Vapour Pressure and Enthalpy of Sublimation of Ferrocene. J. Chem. Thermodynamics, 15, 619.

Table 1

Increase of Smoke-Point Fuel Flowrate  
with Ferrocene Fuel Additive

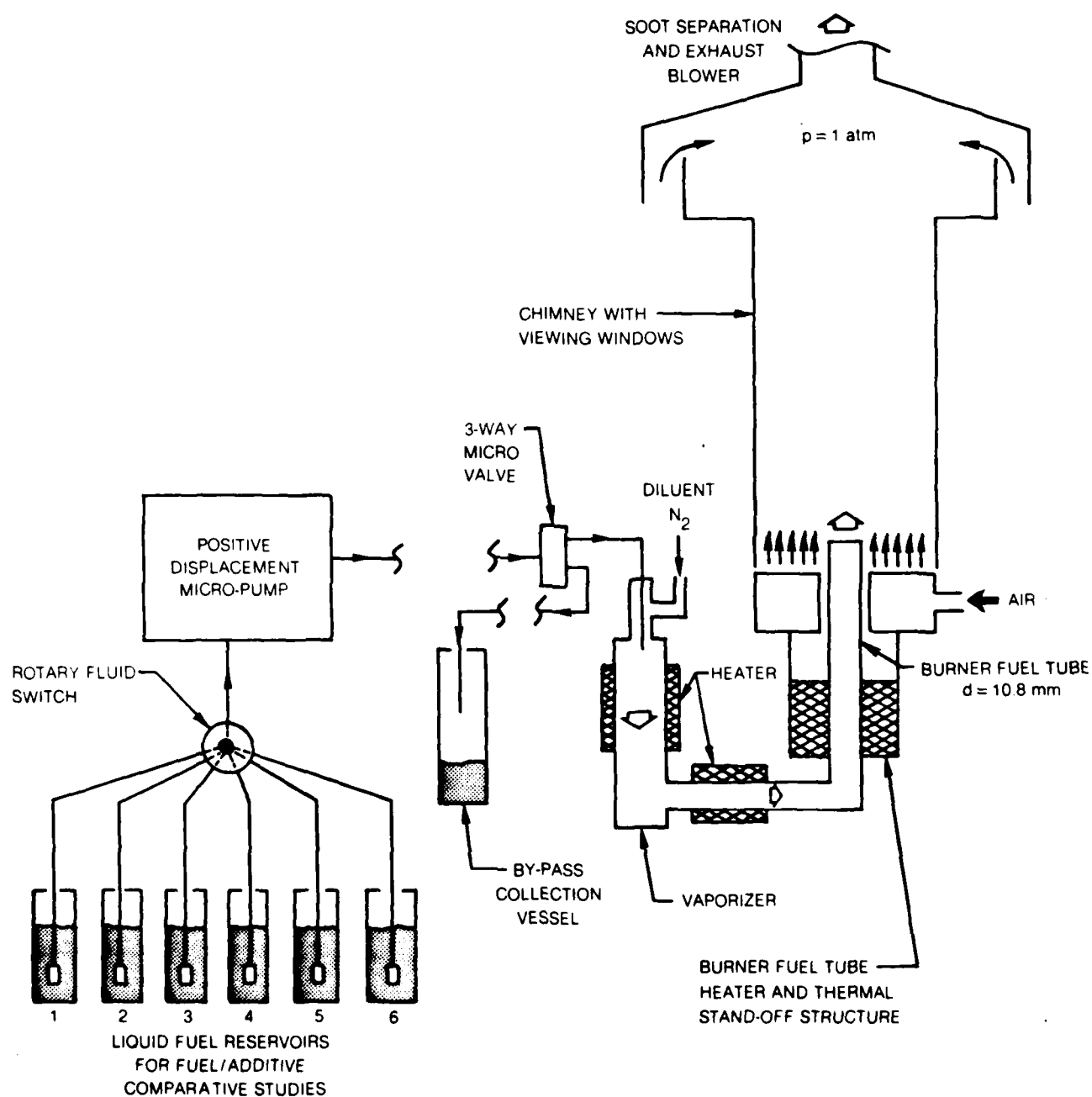
Flame: Diffusion/Pre-Heated Fuel Burner  
Fuel Flowrate Control: Positive Displacement Pump  
N<sub>2</sub> Diluent Flow: Constant Vaporizer Dilution 37 sccm

Ferrocene Concentration wt. %	Smoke-point fuel flowrate - microliters/min		
	20% Toluene/80% Iso-octane		JP4
	T <sub>f</sub> = 100 C	T <sub>f</sub> = 250 C	T <sub>f</sub> = 250 C
0	80	70	85
0.1	90	85	160
0.3	160	150	225



FIG. 1

# STUDIES OF SOOT REDUCTION WITH ADDITIVES TO LIQUID FUELS USING A PRE-HEATED FUEL BURNER



## APPENDIX IV

### PRESENTATIONS/PUBLICATIONS UNDER AFOSR CONTRACT F49620-83-C-0113

#### Presentations

1. "Fuel Additive Effects in Sooting Flames" was presented by P. A. Bonczyk at the 1983 AFOSR Contractor's Meeting on Airbreathing Combustion Dynamics Research, Scottsdale, Az., September 19-22, 1983.
2. P. A. Bonczyk was an invited participant in, "Oxidation Kinetics and Soot Formation," a research review held at NASA Lewis Research Center, Cleveland, Ohio, October 6, 1983.
3. P. A. Bonczyk gave the invited seminar, "In-Situ Laser Measurements of Additive Effects on Soot in Laboratory Diffusion Flames," to the Chemical Engineering Department, Yale Univ., November 17, 1983.
4. P. A. Bonczyk contributed the invited paper, "Fuel Additive Effects in Sooting Flames," in a session entitled "Physics of Particulate Carbon" at the Detroit, Mich. Meeting of the American Physical Society, March 26-30, 1984.
5. "Fuel Additive Effects in Sooting Flames" was presented by P. A. Bonczyk at the 1984 AFOSR/ONR Contractor's Meeting on Airbreathing Combustion Research, Pittsburgh, Pa., June 20-21, 1984.
6. P. A. Bonczyk contributed the poster paper, "Measurement of Metallic Fuel Additive Effects on Soot in Diffusion Flames," at the Twentieth Symposium (Internat.) on Combustion, Ann Arbor, Mich., August 12-17, 1984.
7. P. A. Bonczyk gave the invited presentation, "Effects of Barium and Iron Fuel Additives on Soot in Flames," at the Particulate Emission Technology Meeting, Naval Postgraduate School, Monterey, Calif., April 16-18, 1985.
8. P. A. Bonczyk contributed the paper, "Effects of Alkaline-Earth and Similar Metal Additives on Soot in Flames," at the Eastern Section Combustion Institute Meeting, Philadelphia, Pa., November 4-6, 1985.
9. P. A. Bonczyk gave the invited seminar, "Spectroscopic Studies of Additive Effects on Sooting Flames," to the Chemical Engineering Department, Yale Univ., April 11, 1986.

10. "Fuel Additive Effects in Sooting Flames" was presented by P. A. Bonczyk at the 1986 AFOSR/ONR Contractor's Meeting on Combustion, Stanford Univ., Stanford, Calif., June 18-20, 1986.

#### Publications

1. Bonczyk, P. A.: Fuel Additive Effects in Sooting Flames. Bull. Am. Phys. Soc. 29, 527 (1984).
2. Bonczyk, P. A.: The Influence of Alkaline-Earth Additives on Soot and Hydroxyl Radicals in Diffusion Flames (submitted for publication in COMBUSTION and FLAME).
3. Bonczyk, P. A.: Suppression of Soot in Flames by Alkaline-Earth and Other Metal Additives (submitted for publication in COMBUSTION SCIENCE and TECHNOLOGY).
4. Bonczyk, P. A.: Laser-Induced Saturated Fluorescence of SrOH in a Diffusion Flame (to be submitted for publication in APPLIED OPTICS).

END

10-86

DTIC